

Department of Microbiology, Tumor and Cell Biology (MTC)
Karolinska Institutet, Stockholm, Sweden

DEVELOPMENT OF AUTOMATED FLUORESCENCE MICROSCOPY METHODS TO ASSIST THE DIAGNOSIS AND TREATMENT OF HUMAN MALIGNANCIES

Emilie Flaberg



**Karolinska
Institutet**

Stockholm 2011

Front cover picture:

Extended field mosaic, 16X

Monolayer of human prostate fibroblasts, α -smooth muscle actin-positive (green)

Prostate tumor cells (red) growing on top of fibroblasts

All nuclei stained with Hoechst (blue)

Back cover picture:

Extended field mosaic, 10X + time-lapse imaging (250 time-points)

Unlabelled BjhTERT fibroblast monolayer (phase-contrast)

Five-color projection of trajectories of prostate tumor cells during a 62.5 hour long movie, each color represent a 12.5 hour interval (in order; yellow, green, violet, blue and red)

All previously published papers were reproduced with permission from the publisher.

Published by Karolinska Institutet. Printed by Larserics Digital Print.

© Emilie Flaberg, 2011

ISBN 978-91-7457-466-1

TO EVERYONE CURIOUS

Somewhere, something incredible is waiting to be known
- Carl Sagan

ABSTRACT

Fluorescence microscopy is a powerful technique used in many biological laboratories. It is often used as an illustrative tool but in combination with manual efforts, valuable quantitative results can also be obtained. The potential of automated fluorescence microscopy has been clearly shown by the high-content and high throughput studies performed in the pharmaceutical industry and more recently in specialized high throughput imaging facilities. Computer controlled image capture and analysis not only scales up the actual image capture process and data production it also brings an important level of objectiveness into microscopy, a field otherwise suffering from an inherent human bias in the selection of which objects to study. There is a growing need for the technique to be available for “everyone”, as a regular microscopy tool in biological laboratories.

This thesis illustrates that the combination of available and affordable techniques allow us to develop automated microscopy methods, including automated capture and image analysis routines that can be applied to answer different biological questions. We show that a visual programming language enable us to make flexible applications for automated microscopy, without detailed knowledge of complex computer languages (Paper I, Paper III - Paper VI).

Using our automated fluorescence imaging and analysis method, in combination with a fluid dispenser robot for drug printing, we have developed an assay for high throughput drug sensitivity testing. In Paper III, we studied the effect of 29 different cytostatic drugs on 17 different lymphoblastoid cell lines. These cell lines are good *in vitro* models for the post-transplant lymphoproliferative disease (PTLD), and the aim of this study was to characterize which drugs would be optimal in the treatment of these patients. Summarizing the effect of each drug on all 17 LCLs, we identified epirubicin and paclitaxel as drugs that were highly effective (even at low concentrations). The same microscopy method was applied in combination with an analysis program that could identify and count differentially labelled cells in co-cultures. Using this approach, we could characterize which cytostatic drugs affect NK cell cytotoxicity negatively (Paper IV). Our data suggested that chemotherapy protocols including proteasome inhibitors (such as bortezomib) or anti-microtubule drugs (paclitaxel, docetaxel and vinblastine) may interfere with NK cell-based immunotherapy, if applied simultaneously. Taken together, these two studies suggested that our drug sensitivity test might prove useful in assisting the design of optimal and individualized treatment protocols for cancer patients.

In Paper V and VI, we have applied the technique in an approach to study neighbour suppression by fibroblasts on tumor cell proliferation, in an attempt to mimic *in vitro* a possible microenvironmental control function *in vivo*. These two studies demonstrated that the culture of tumor cells on monolayer of primary fibroblasts, might lead to either growth stimulation or growth inhibition of tumor cells. Fibroblasts derived from the prostate of patients diagnosed with prostate carcinoma (potential CAFs) were the least inhibiting, and occasionally even promoting tumor cell proliferation. However, fibroblasts derived from the skin of pediatric patients were highly represented in the group of the most inhibitory fibroblasts. Our high-throughput study, with over 500 heterotypic cell combinations, with four independent measurements for each sample and individual counting of each tumor cell, indicated that the effect of fibroblasts on tumor cell proliferation was predominantly inhibitory. The technique allowed us to identify fibroblasts with consistently high and with consistently low inhibitory capacity. These are valuable fibroblasts to use in further studies to understand the mechanism behind inhibition and its possible clinical relevance. In Paper VI we specifically investigated the role of the structure of the fibroblast monolayer. We

found that it was clearly not sufficient to have the inhibitory fibroblasts present in the mixed cell culture but that they also had to form a confluent and sufficiently matured, intact monolayer to exert the inhibitory effect. Our data suggested that structured accumulation and deposition of extracellular matrix molecules might provide orientation dependent behavioral cues to the tumor cell in an un-manipulated, inhibitory monolayer. Preliminary gene profiling suggested multiple differences in the signature of inhibitory and non-inhibitory fibroblasts.

LIST OF PUBLICATIONS

This thesis is based on the following (original) papers, which are referred to in the text by their Roman numerals:

METHOD DEVELOPMENT

- I. **Emilie Flaberg**, Per Sabelström, Christer Strandh, Laszlo Szekely. **Extended Field Laser Confocal Microscopy (EFLCM): Combining automated Gigapixel image capture with *in silico* virtual microscopy**. BMC Medical Imaging (Technical advances). 2008 Jul 16;8:13
- II. **Emilie Flaberg**, György Stuber, Laszlo Szekely. **Multi-dimensional laser confocal microscopy on live cells in submicroliter volumes using glass capillaries** Acta Histochem Cytochem. Technical advances. 2006 Aug 30;39(4):103-6. Epub 2006 Jun 2.

APPLICATIONS 1 – DRUG SENSITIVITY ASSAYS

- III. Laszlo Markasz, György Stuber, **Emilie Flaberg**, Åsa Gustafsson Jernberg, Staffan Eksborg, Eva Olah, Henriette Skribek, Laszlo Szekely. **Cytotoxic drug sensitivity of Epstein-Barr virus transformed lymphoblastoid B-cells** BMC Cancer. 2006 Nov 13;6:265.
- IV. Laszlo Markasz, György Stuber, Bruno Vanherberghen, **Emilie Flaberg**, Eva Olah, Ennio Carbone, Eva Klein, Henriette Skribek, Laszlo Szekely. **Effect of frequently used chemotherapeutic drugs on cytotoxic activity of human Natural Killer cells**, Mol Cancer Ther. 2007 Feb;6(2):644-54.

APPLICATIONS 2 – FIBROBLAST and TUMOR CELL ASSAYS

- V. **Emilie Flaberg**, Laszlo Markasz, Gabor Petranyi, Gyorgy Stuber, Ferenc Dicső, Nidal Alchihabi, Èva Oláh, István Csízy, Tamás Józsa, Ove Andrén, Jan-Erik Johansson, Swen-Olof Andersson, George Klein, Laszlo Szekely. **High-throughput live-cell imaging reveals differential inhibition of tumor cell proliferation by human fibroblasts**. Int J Cancer. 2011 Jun 15;128(12):2793-802. doi: 10.1002/ijc.25612. Epub 2010 Dec 29
- VI. **Emilie Flaberg**, Hayrettin Guven, Andrii Savchenko, Tatiana Pavlova, Vladimir Kashuba, Laszlo Szekely & George Klein. **The differential inhibition of tumor cells by normal and cancer-derived fibroblasts is dependent on the architecture of the fibroblast monolayer**. Manuscript

RELATED PUBLICATIONS

Xianghua Zhou, Fei Tian, Johan Sandzen, **Emilie Flaberg**, Laszlo Szekely, Renhai Cao, Yihai Cao, Claes Ohlsson, Martin O. Bergö, Jan Borén, Levent M. Akyürek. **Disruption of filamin B is essential to early mouse development and leads to impaired microvasculature and vertebral malformations** Proc Natl Acad Sci U S A. 2007 Mar 6;104(10):3919-24. Epub 2007 Feb 26.

György Stuber, Karin Mattsson, **Emilie Flaberg**, Kati E, Laszlo Markasz, Sheldon JA, Georg Klein, Schultz TF, Laszlo Szekely. **HHV-8 encoded LANA-1 alters the higher organization of the cell nucleus**. Mol Cancer. Published 2007 Apr 13;6:28.

Laszlo Markasz, Lorand Levente Kis, György Stuber, **Emilie Flaberg**, Rita Otvos, Staffan Eksborg, Henriette Skribek, Eva Olah, Laszlo Szekely. **Hodgkin-lymphoma-derived cells show high sensitivity to dactinomycin and paclitaxel**. Leuk Lymphoma. Published 2007 Sep;48(9):1835-45

Laszlo Markasz, Henriette Skribek, Michael Uhlin, Rita Otvos, **Emilie Flaberg**, Staffan Eksborg, Eva Olah, Gyorgy Stuber, Laszlo Szekely. **Effect of frequently used chemotherapeutic drugs on cytotoxic activity of human cytotoxic T- lymphocytes**. Journal of Immunotherapy. 2008 Apr;31(3):283-93.

Laszlo Markasz, Bruno Vanherberghen, **Emilie Flaberg**, Rita Otvös, György Stuber, Åsa Gustafsson Jernberg, Eva Olah, Henriette Skribek, Laszlo Szekely. **NK cell-mediated lysis is essential to kill Epstein-Barr virus transformed lymphoblastoid B cells when using rituximab**. Biomed Pharmacother. 2008 Sep 30.

Stuber György, **Flaberg Emilie**, Petranyi Gabor, Otvos Rita, Rokaeus Nina, Kashuba Elena, Wiman Klas G, Klein Georg, Szekely Laszlo. **PRIMA-1MET induces nucleolar translocation of Epstein-Barr virus-encoded EBNA-5 protein**. Mol Cancer. 2009 Mar 26;8(1):23.

Eriksson Sofi E, Prast-Nielsen Stefanie, **Flaberg Emilie**, Szekely Laszlo, Arnér Elias S.J. **High levels of thioredoxin reductase 1 modulate drug-specific cytotoxic efficacy**. Free Radic Biol Med. 2009 Dec 1;47(11):1661-71

Skribek H, Otvos R, **Flaberg Emilie**, Nagy N, Markasz L, Eksborg S, Masszi T, Kozma A, Adam E, Miseta A, Klein E, Szekely L. **Chronic lymphoid leukemia cells are highly sensitive to the combination of prednisolone and daunorubicin, but much less to doxorubicin or epirubicin**. Exp Hematol. 2010 Dec;38(12):1219-30. Epub 2010 Sep 15.

Otvos R, Skribek H, Kis LL, Gloghini A, Markasz L, **Flaberg Emilie**, Eksborg S, Konya A J, Gergely L, Carbone A, Szekely L. **Drug sensitivity pattern of HHV8 carrying body cavity lymphoma cell lines**. BMC Cancer. 2011 Oct 12;11(1):441.

CONTENTS

1. AIMS OF THESIS	1
1.1 METHOD DEVELOPMENT	1
1.2 METHOD APPLICATIONS	1
2. INTRODUCTION	2
2.1 AUTOMATION IN SCIENCE	2
2.2 LIGHT MICROSCOPY TECHNIQUES	3
2.2.1 BRIGHT FIELD MICROSCOPY	4
2.2.2 PHASE-CONTRAST MICROSCOPY	4
2.2.3 FLUORESCENCE MICROSCOPY	4
2.2.4 CONFOCAL MICROSCOPY	6
2.3 AUTOMATED MICROSCOPY/HIGH THROUGHPUT IMAGING	7
2.4 DIGITAL IMAGING AND IMAGE ANALYSIS	9
2.4.1 SOFTWARE ENVIRONMENT TO CREATE IMAGE CAPTURE AND PROCESSING TOOLS	10
2.5 CANCER	10
2.5.1 WHY DO WE GET CANCER?	10
2.5.2 NORMAL STROMA VERSUS TUMOR STROMA	13
2.5.3 TUMOR MICROENVIRONMENTAL CONTROL – WHY DON’T WE ALL GET CANCER?	15
2.6 DRUG SENSITIVITY ASSAYS	16
2.6.1 HOW CAN WE FIND THE BEST DRUG FOR ONE PATIENT	16
3. RESULTS AND DISCUSSION	19
MICROSCOPY SYSTEMS	19
3.1 PAPER I	20
3.2 PAPER II	24
3.3 PAPER III	25
3.4 PAPER IV	27
3.5 PAPER V	28
3.6 PAPER VI	32
5. CONCLUDING REMARKS AND FUTURE PERSPECTIVES	35
6. METHODOLOGICAL CONSIDERATIONS	37
6.1 PRIMARY FIBROBLAST CULTURES – TRICKS AND TIPS	37
6.2 PROGRAMMING IN OPENLAB AUTOMATOR – NUTS AND BOLTS	37
6.3 IMAGE PROCESSING/ANALYSIS - COMMENTS	38
7. ACKNOWLEDGEMENTS	40
8. REFERENCES	42

LIST OF ABBREVIATIONS

AIDS	acquired immune deficiency syndrome
ARL	AIDS related lymphoma
CAF	cancer associated fibroblast
CCD	charge coupled device
CLL	chronic lymphoid leukemia
CSU	confocal scanner unit
EBV	Epstein Barr virus
ECM	extracellular matrix
EFLCM	extended field laser confocal microscopy
EGF	epidermal growth factor
EGFP	enhanced green fluorescent protein
EGFR	epidermal growth factor receptor
EMT	epithelial mesenchymal transition
F	false
FBS	fetal bovine serum
FGM	fibroblast growth medium
FGS	fibroblast growth supplement
FMCA	fluorometric microculture cytotoxicity assay
FSP-1	fibroblast specific protein-1
GFP	green fluorescent protein
IMDM	Iscoe's modified Dulbecco's medium
LCL	lymphoblastoid cell line
MMP	matrix metalloproteinase
mRFP	monomeric red fluorescent protein
MTT	3-(4,5-Dimethylthiazol-2-yl)-2,5-diphenyltetrazolium bromide
NA	numerical aperture
NG2	neuron-glial antigen-2
NK	natural killer
NSC	Nipkow spinning disc
OME	open microscopy environment
PBS	phosphate buffered saline
PCR	polymerase chain reaction
PDGFR	platelet derived growth factor receptor

PMT	photomultiplier tube
POC	perfusion open closed
PSG	penicillin, streptomycin and gentamicin
PTLD	post-transplant lymphoproliferative disease
RAM	random access memory
SMA	smooth muscle actin
SNR	signal to noise
SPSC	single point scanning confocal
T	true
TGF	transforming growth factor
VEGF	vascular endothelial growth factor

1. AIMS OF THESIS

1.1 METHOD DEVELOPMENT

The first aim of this project was to set-up an automated microscopy platform that was robust and flexible enough to run different types of fluorescence based experiments. Using a visual programming language and image analysis software, we set out to develop programs that could control the microscope hardware and perform automated image capture and image analysis. The objective throughout this work was to implement and adjust the method in different projects in order to answer specific tumor-biological questions, using automated microscopy.

1.2 METHOD APPLICATIONS

The technique was specifically adapted for automated imaging and analysis of cells in 384-well plates. The goal was to develop an automated drug sensitivity assay that could measure the effects of cytostatic drugs on tumor cell viability and on NK cell cytotoxicity.

The final aim of this thesis was to characterize the effect of human primary fibroblasts on tumor cell proliferation. Using our automated microscopy platform the goal was to optimize the technique to measure the proliferation of tumor cells, over time, in co-culture with a large panel of primary human fibroblasts.

2. INTRODUCTION

“...biology is undergoing this remarkable transformation from being a purely laboratory-based science, where each individual work on his or her project, to be an information-based science that involves the integration of vast amounts of data across the whole world and trying to learn things from this tremendous data set” (Lander 2004)

2.1 AUTOMATION IN SCIENCE

Automated data collection is responsible for a conceptual shift in the science of biology. High-throughput methods are not only transforming biology by their production of large amounts of new scientific knowledge but also because the technique itself, with the production of giant sets of data, changes the requirements on how scientists handle, interpret, describe and report data (King, Rowland et al. 2009). The bottleneck is no longer the production of experimental data but the actual interpretation of them. We are now completely dependent on powerful computers in order to store, process the data and to carry out meaningful analysis. The development of new high throughput imaging techniques of biological materials is based on the recent development in computational processing power, memory handling and data storage capacity (Gonzalez and Woods 2008). There are now many examples of successful implementation of high throughput techniques, demonstrating their potential, not at least regarding its cost effectiveness. A stunning example is found in the reductions in DNA sequencing costs over the last ten years. From October 2008 until July 2011 the cost per genome dropped from 8 million USD to 10 000 USD, due to new high throughput technology (Wetterstrand 2011).

Technical advancements continuously open up new ways how experiments can be performed. It is now possible to collect millions of images of cells “blindly” and develop hypothesis based on *in silico* created patterns found by (for example) automated image analysis and cluster analysis. The acquisition of new knowledge is no longer limited to the traditional way of scientific inquiry that is based on the scheme of i) observation, ii) formulation of hypothesis and iii) test the hypothesis by experiment. Certainly the basis of science is still the hypothetico-deductive method and the recording of experiments in sufficient detail to enable reproducibility, but it does not necessarily need to be in that order. New machine learning tools that have access to large datasets, of both experimental data and accumulated knowledge produced by the scientific community, will be able to find new correlations, reveal cause and effect relationships in an automated fashion. The creation of the first robot scientist Adam, suggested that a computer driven system could formulate specific hypothesis upon being initiated by vague instructions by mining large databases. Subsequently the system could design and execute experiments to test the series of hypotheses, evaluate the results, refine the hypotheses and carry out additional experiments that prove or disprove the first set of hypotheses (King, Rowland et al. 2009).

The role of the new generation of scientists will be to design and implement new ways to collect reliable raw data on one hand and to extract intellectually meaningful and practically useful conclusions on the other hand. Today we witness a revolution where powerful new algorithms step-by-step disqualify the various objections against the limits of artificial intelligence, among other the famous Lady Lovelace’s Objection that states that computers are incapable of originality because machines are incapable of independent learning (“*The*

Analytical Engine has no pretensions whatever to originate anything. It can do whatever we know how to order it to perform. It can follow analysis; but it has no power of anticipating any analytical relations or truths”- Ada Lovelace 1815-1852) (King, Rowland et al. 2009).

Computers are now able to extract natural laws from raw experimental data in a similar way as Kepler’s laws of planetary movements were formulated on the basis of astronomical observations (Schmidt and Lipson 2009).

2.2 LIGHT MICROSCOPY TECHNIQUES

Collection of data in this thesis is primarily done using different types of light microscopy techniques. The name of the technique is revealing, it originates from the Greek; μικρός (*mikrós*) σκοπεῖν (*skopeín*) and can be translated: “to look at small things”. The light microscope is an instrument that uses light and lenses to magnify objects that are not possible to see with the naked eye. The various light microscopes available for general and specialized use in research are all compound microscopes, using multiple lenses for magnification. In comparison, a magnifying glass, the simplest form of a microscope, uses only one lens. Resolution of a system defines the distance of how close two objects can be and still be seen as two separate entities. The resolving power of the human eye is 0,2 mm and is determined by the spacing of the photoreceptor cells in the retina. Apart from helping us to see small things - the job for a microscope is to improve resolution and contrast. The theoretical resolution of a light microscope is 0,2 μm , improving human vision by 1000 times (Ross, Kaye et al. 2002). In microscopy, resolution is determined by the diffraction of light, as postulated by Ernst Abbe in 1873 (Chi 2009) (Figure 2.1). Resolution depends on the light gathering capacity of the lens (defined as the numerical aperture of the objective (NA)) and the wavelength of the light.

$$\text{Resolution (simplified)} = \frac{\text{Wavelength of light } (\lambda)}{2 \times \text{Numerical aperture (NA)}}$$

Figure 2.1 Abbe’s law

Thus, resolution gets better with high NA objectives and short wavelengths of light. Magnification itself does not contribute to resolution, even though it is often so that objectives with high magnification also have high NA. Magnification increases the apparent size of an object and affects its intensity. The brightness of an image is proportional to the NA and inversely proportional to magnification (North 2006; Goldman, Swedlow et al. 2010). The thickness of the imaging plane (the depth of focus) gets thinner with high NA-objectives (Conchello and Lichtman 2005). In the last two decades advancement in applied physics has circumvent the limitations of diffraction-limited resolution and it is now possible to study object smaller than 20-50 nm (Hell and Wichmann 1994; Gustafsson 2000; Heintzmann, Jovin et al. 2002). Perhaps there is no other single device that brought so much to biology as the microscope. Since 1675, when Anton van Leeuwenhoek first discovered the cells and bacteria under its lenses, until today when we can study the proteins inside living cells at the nanometer scale (Eggeling, Ringemann et al. 2009).

The work in this thesis is based on three types of light microscopy techniques: bright-field, phase contrast and fluorescence microscopy.

2.2.1 Bright field microscopy

In conventional bright-field microscopy the sample is illuminated with transmitted white light. The image is the result of different absorption levels of light and light scattering throughout the sample, either due to density differences in structures or due to histological staining of the specimen. Contrast and quality is limited by the thickness of the sample.

2.2.2 Phase-contrast microscopy

Phase-contrast microscopy shows proportional differences in optical density in a sample. It converts sample-induced shifts in the phase of light, to visible intensity differences. The transmitted light will be phase-shifted in the sample due to differences in the refractive index. Imposed phase shift in the transmitted light will interfere with the diffracted light resulting in the phase contrast image. A phase contrast image show higher contrast than a bright-field image but the quality is more limited by the thickness of the sample.

2.2.3 Fluorescence microscopy

Fluorescence microscopy allows the visualization of specific and selected structures within a sample. The technique is based on the activation of molecules with fluorescence capabilities (fluorophores) that have been tagged to structures of interest (Haugland 2005). Fluorophores have chromophoric units with electrons organized in such a way that they favour the absorption of certain wavelengths of lights. Upon illumination, electrons in the chromophoric unit absorb photons with certain energy and will move from their ground state to a higher energy level and create a molecule in an excited state. The excited lifetime is extremely short and the electrons will fall back down to their ground state emitting the excess energy as fluorescence light. Due to energy loss in form of vibration in the excited state, the energy of the emitted light will be slightly less and having a longer wavelength than the excitation light. The difference between the exciting and emitted wavelengths, known as the Stokes shift, is the critical property that makes fluorescence microscopy so powerful (Lichtman and Conchello 2005; Wolf 2007) (Figure 2.2).

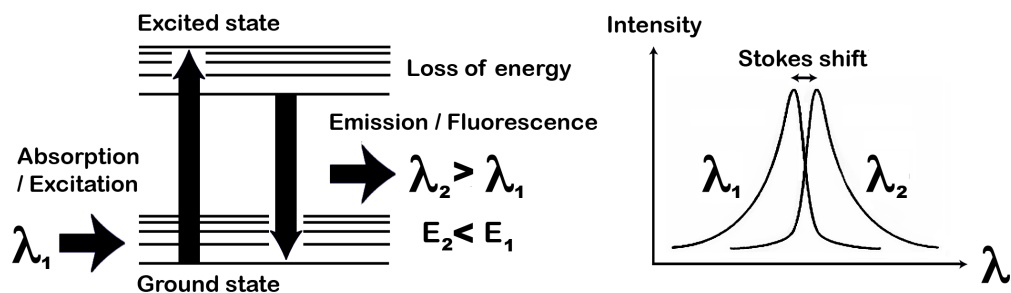


Figure 2.2 Jablonski energy diagram, simplified (left). Fluorophore absorption and emission profiles, with Stokes shift (right).

Under optimal settings, using matching excitation light and fluorophores in combination with proper filter set-ups, it is possible to filter out excitation light without blocking emitted fluorescence and to see only objects that are fluorescent. Contrast is therefore higher in fluorescence microscopy compared to the absorption techniques, such as bright field and phase contrast (Lichtman and Conchello 2005). Fluorescence intensity is proportional to the number of fluorophores in the excited state and to the illumination intensity. However, the excited state and the fluorescence intensity can be saturated with increasing illumination intensity (Wolf 2007). Photobleaching is a common phenomenon and potential problem in

fluorescence microscopy and it is therefore important to minimize both the illumination intensity and its duration. Shut off illumination when it is not needed. Anti-fading agents can also be applied to the sample during the staining procedure.

Fluorophores can be added to the specimen in essentially three ways: (i) conjugated to antibodies that bind to specific targets, (ii) be part of dyes having inherent specific binding (such as nucleic acid stains like Hoechst and DAPI), or (iii) through the introduction of fluorescent proteins genetically encoded as a fusion with a cDNA of interest (Lippincott-Schwartz and Patterson 2003). The discovery and cloning of GFP, the green fluorescent protein, found in the *Aquaria Victoria* jellyfish (Shimomura, Johnson et al. 1962; Prasher, Eckenrode et al. 1992) was the starting point for a production and exploration of numerous fluorescent proteins with colors that span the whole visible spectrum (Goldman, Swedlow et al. 2010). One of these was the red fluorescent protein (DsRed), which was isolated from the coral *Discosoma*. The problems associated with its wild-type tetramer form has recently been overcome and its monomeric descendant, mRFP (monomeric red fluorescent protein), is together with GFP valuable tools of cell biology, especially in live cell imaging. mRFP has minimal emission when excited at wavelengths optimal for GFP which makes these two fluorescent protein optimal for multicolor labeling (Campbell, Tour et al. 2002). Fluorescent proteins are, because of their endogenous expression, very suitable for live cell imaging. Fluorescent lipid molecules and organelle-specific dyes that are cell permeable and compatible with living cells are other alternatives for live cell staining (Stephens and Allan 2003). We have used various labelling techniques; genetic (EGFP and mRFP fusion proteins) and chemical organelle-specific dyes (such as Mitotracker or Lysotracker) to ascertain the viability and functional integrity of our cells during the experiments presented in this thesis (Figure 2.3).

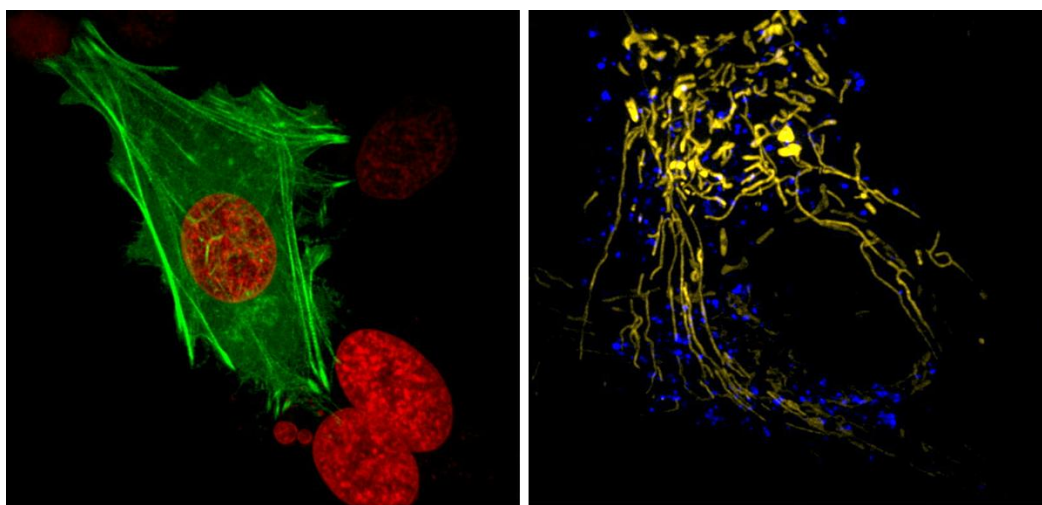


Figure 2.3 Visualization of cellular organelles in living cells over an extended period of observation (4 dimensional, confocal time-lapse movies, POC-mini chamber). EGFP-actin (green) and mRFP-histone H2A (red) in transfected PC3 prostate carcinoma cells, 63X (left). Organelle staining of mitochondria (Mitotracker, yellow) and lysosomes (Lysotracker, blue) in a human fibroblast, 100X (right).

When working with living cells it is necessary to consider the viability of cells on the microscope stage. The energy of photons can cause photodamage and cells are particularly sensitive to illumination in the presence of fluorophores, which generate free radicals upon photobleaching. Again, limiting the illumination time is vitally important but there are also other ways of limiting light-induced damage. Reducing the levels of oxygen and supplementing the medium with scavengers such as ascorbic acid (vitamin C) are other ways to limit the reactions with oxygen free radicals. It is also important to keep the cellular

environment stable, controlling factors such as temperature, pH, CO₂ and humidity (Stephens and Allan 2003; Frigault, Lacoste et al. 2009).

Wide field fluorescence microscopy provides clear lateral (x- and y-axis) information but only limited axial (z-axis) information (North 2006). Because fluorescence light is collected from the entire depth of the specimen, the resulting image is the sum of fluorescence signals in focus together with un-sharp, out-of-focus signals. For samples thicker than a few micrometer or when detailed axial information is needed (for co-localization) other techniques will be more optimal to use (see confocal microscopy 2.2.4) (White, Amos et al. 1987). Deconvolution, a computational technique that restores z-axis information based on properties of the imaging system, is an often used and effective way to improve the quality.

Fluorescence microscopy has revolutionized biological imaging, allowing scientists to study specific structures, organelles and proteins both inside living and in fixed cells and tissues. The result is an amazing world of cellular details – although in an artificially coloured cell universe.

2.2.4 Confocal microscopy

Confocal microscopy allows the visualization of thin optical sections of a specimen with minimal out of focus blur. A series of sections along the z-axis can be collected in order to build a Z-stack, which can be rendered to represent a 3D view of the object. The way light behaves when it passes through the lenses in a microscope contributes to diffraction-limited resolution. Not even illumination of an infinitely small point, that emits fluorescence light, will produce an image of a perfect point. The product is rather a blurred point with a “halo”. This is called the “Airy disk” and is the result of diffraction of light. The diffraction of light does not only have an affect in the xy-direction but also in the z-direction. The Airy disk extends in the z-direction as an hourglass shaped light cone. It is the “tails” of this hourglass that are reduced using confocal microscopy, restricting the collected fluorescent signal to one focus plane (Conchello and Lichtman 2005; Inoue 2006). Lasers, with their coherent and narrow beam of light, are used as excitation sources and are scanned as a focused point across the sample. The emitted fluorescence is collected through a pinhole before reaching the detector. The pinhole allows only light predominantly from the focal plane to reach the detector, while rejecting the out-of-focus photons (Lucitti and Dickinson 2006).

Conventional single-point scanning confocal (SPSC) systems uses one pinhole to exclude the out-of-focus fluorescence from above and below the sample focus plane (Hammond and Glick 2000). The sample is imaged using a single laser beam, focused to a spot that scans across the sample. A 2D image is sequentially built up from the point-by-point emitted fluorescence and collected through the confocal pinhole and registered by a photomultiplier tube (PMT). The scanning time for one image is proportional to the exposure time at each point (pixel dwell time) and the total number of points (size of the image). This scanning process is thus limited by the exposure time, (typically in the microsecond range) needed to collect sufficient amount of fluorescence. Shorter exposure times have to be compensated for by increased illumination.

Nipkow spinning disc systems (NSC) parallelize the point scanning process and uses CCD camera for detection of an instant confocal image. The confocal microscopy work presented in this thesis is produced using Yokogawa Nipkow spinning disc systems. Instead of one pinhole, the Yokogawa scanning head (CSU10 and CSU22) has twenty thousand pinholes with matching microlenses, producing focused multi-beam illumination and parallelized confocal point detection with instant confocal imaging. To overcome the poor transmission of the first versions of scanning discs, Yokogawa introduced the microlens-array disc and

achieved up to 40% better transmission (Wang, Babbey et al. 2005). The pinholes are arranged in such a pattern that when the disc rotates, a given point in the sample is illuminated several hundred times per second, allowing lower excitation intensities than compared to SPSC systems. Because the intensity in each spot is low and the effective quantum efficiency of the CCD camera is higher than that of the photomultiplier tube, disk scanners cause less photobleaching and less phototoxicity than SPSC systems (Wang, Babbey et al. 2005; Hardin 2006). Wang et al. have shown that the CSU10 system was capable of reproducing the highest SNR (signal-to-noise ratio) measured for an SPSC system at approximately $1/15^{\text{th}}$ of the rate of photobleaching. Perhaps the only drawback of the spinning disc parallelization is that the axial resolution is slightly compromised due to cross-talk between the high-density foci; $0,71\text{ }\mu\text{m}$ compared to $0,60\text{ }\mu\text{m}$ for the SPSC system (100X/NA1.4) (Egner 2002; Wang, Babbey et al. 2005).

2.3 AUTOMATED MICROSCOPY/HIGH THROUGHPUT IMAGING

High-throughput techniques have defined the development of modern biology, from flow and laser scanning cytometry (cell counting/surface molecule analysis), mass spectrometry (protein analysis), microarrays (DNA or protein profiling) to whole genome sequencing techniques. Microscopy and imaging has also undergone a transformation towards automation, and moved from its traditional purely descriptive function into becoming an effective quantitative tool. Line scanners, using transmitted light illumination and a linear array of detectors, creating a number of contiguous overlapping image stripes paved the way for automated microscopy in pathology. Techniques aiming at the digitization of entire microscope slides have led to the emergence of virtual histopathology (Ying and Monticello 2006). Automated, bias free image capture of large amount of consecutive image tiles and the alignment of them into a continuous panorama, which is freely "zoomable" *in silico* is the foundation of virtual microscopy (Leong and McGee 2001; Lundin, Lundin et al. 2004; Lee 2005; Glatz-Krieger, Spornitz et al. 2006). Automated fluorescence microscopy at low resolution is emerging as an alternative to laser scanning cytometers (Varga, Bocsi et al. 2004). More recently the emergence of the tissue microarray technology has facilitated the visualization and analysis of molecular alterations in thousands of tissue specimens in a parallel fashion (Kallioniemi, Wagner et al. 2001; Lundberg, Gry et al. 2008).

The time consuming manual microscopy process and the main dilemma in traditional microscopy - the inherent human bias in the selection of an image area, has been overcome. Meanwhile, a demand for automated, high-resolution, fluorescence microscopy techniques has been growing, to match the development the other techniques, and to allow quantitative analysis of fluorescence properties (Pepperkok and Ellenberg 2006). The hardware prerequisites for such automatic imaging systems are (1) motorization of the microscope stage, (2) automatic changing of objectives and/or laser scanner zoom, and (3) switching of fluorescence filter and/or laser lines (Conrad, Wunsche et al. 2011). Standard microscopes are now being replaced with new purpose-built platforms that enable collection of high-spatial and high-temporal resolution data (Barbe, Lundberg et al. 2008; Lundberg, Gry et al. 2008; Dobbie, King et al. 2011).

High-throughput imaging systems should ideally be compatible with many fluorescence-based assays and they should be completely adapted in terms of both hardware and software for fully automated operation (Pepperkok and Ellenberg 2006). Commercial systems are often forced to focus on specific aims; ultra-high throughput with limitations in magnification and wave-lengths, adaptable for plates and fixed cells on slides but not for living cells in chambers, and image analysis restricted to certain processes and measurements. The advent of new automated systems with an open software architecture

that allow users to develop their own tailor made modules for both capturing and image analysis has opened up new ways of performing automated microscopy. A feature of the development of a new digital technology, by different microscope manufacturers, was the emergence of large number of different digital image formats. Meaningful comparison of data from different laboratories on the other hand require standardized handling of digital image information. The reaction of the scientific community to this confusion of multiple-formats was the creation of “The Open Microscopy Environment (OME)”. It is part of a multi-site collaborative effort among academic laboratories and a number of commercial entities to produce open tools to support data management for biological microscopy research (Swedlow 2011).



Figure 2.4 Early high-throughput microscopy. “A scientific conversazione with microscopes provided to view microscopic objects. Such events attracted a large public” (Oheim 2007). Engraving from Illustrated London News 28 April 1855. With permission, Shropshire Museums.

Automated microscopy and high throughput imaging is still challenging and under constant development. Scaling up quantitative microscopy for high-content and true high-throughput screening requires the seamless integration of several advanced techniques, apart from the automated image capture. It is important to consider the need to automate certain steps in the process, such as sample collection and preparation, liquid handling with robotics and the handling of the produced data. Automated image analysis is perhaps the most crucial and challenging part. Despite the extensive literature on pattern recognition and image segmentation, the expertise has only sporadically made its way into the analysis of microscopic images in biological research (Oheim 2007). Recently developed techniques takes automated imaging further, towards a transition to intelligent microscopy. It provides a machine learning-based module that can be trained by the user to automatically identify desired cell states during an unattended, fast, low-resolution pre-scanning mode. Upon identification of a cell of interest it can prompt the imaging system to switch mode and run a desired high-resolution and high-information-content assay (Conrad, Erfle et al. 2004; Conrad, Wunsche et al. 2011). Automated fluorescence microscopy, cell microarray platforms, quantitative image analysis and data mining, combined with multivariate

statistics and computational modeling, now coalesce to produce a new research strategy called systems microscopy (Lock and Stromblad 2010).

One crucial question remains: will automated microscopy continue to mainly be part of consortia and imaging centers that combine transversal expertise in a tight and large-scale academic-industrial partnership, or will it, via commercial products, or clever and highly available (open source) resources make its way into the small- and medium-sized laboratories, to fundamentally change the way fluorescence imaging is done today in cell biological research? (Oheim 2007). There is clearly a gap to fill - the every day need for efficient and objective image capturing in university research labs by researchers with limited funding.

2.4 DIGITAL IMAGING AND IMAGE ANALYSIS

A digital image is a two dimensional array of elements called pixels. The size of each pixel and the total number of pixels in an image is dependent on the detector used. In fluorescence microscopy it is most common to use cold CCD cameras as the signal-collecting sensor. A CCD camera works as an analog to digital converter, converting photons to electrons and the value of each pixel corresponds to the number of photons collected. The dynamic range of a camera defines the capacity to describe different intensities of signals, a 12 bit camera can display 4 096 grey levels.

A basic concept for communication of any kind of information is that received signal equals information plus noise, and this is also true regarding images (Fiske 1990). The first step in image processing is therefore trying to compensate for noise; defects, imperfections, and non-uniformity in the detection (Lo and Puchalski 2008). The aim is to enhance the information component of the signal and to reduce the background. There are many techniques to reduce background, enhance image quality and automatically analyze objects. Below, I will briefly go through some of the most important techniques used in this thesis.

Spatial domain processing refers to image processing based on direct manipulation of pixels in the image plane. There are two types of categories of spatial domain image processing, intensity transformations and spatial filtering. Intensity transformations, such as contrast manipulation and image thresholding operate on single pixels of an image (point processing). Spatial filtering techniques perform operations regarding pixels as correlated entities, working in a neighbourhood of every pixel in an image (neighbourhood processing) (Gonzalez and Woods 2008).

Random noise can be defined as sharp intensity transitions. A smoothing filter effectively reduces such noise by replacing every pixel in the image by the average of the intensities levels in a neighbourhood, defined by the size of a filter mask. However, if it is important to keep edges of objects intact it is better to use a median filter, which works as a good noise-reducer but with less blurring effect than smoothing filters. A median filter rank the pixel values contained in a defined neighbourhood and replaces the central value with the median (no new pixels values are created). In contrast to smoothing and median filters, sharpening filters highlight transitions in intensity and such filters are extensively used for segmentation of objects (Gonzalez and Woods 2008). To separate objects that are touching each other is difficult and a constant challenge in image analysis. Watershed algorithms are a powerful tool for segmentation (Ross 2011). Point-processing using thresholding sets lower and upper threshold values, segmenting the image into features of interest and background, creating a binary image. This tool can be used to select objects for quantification. To remove smooth continuous backgrounds, a rolling ball background subtraction tool can be used. Here, the

image is viewed as a 3D-surface with pixel intensity values interpreted as height values over the xy-plane. A structure element, a ball in this case, is rolled across the 3D-surface and dependent on its radius it will remove background by flatten out the valleys where it cannot reach the lowest points (Gonzalez and Woods 2008). A find maxima tool can be used to quantify point-like objects, by determining local maxima of objects (defined by a noise tolerance that stand out from the background with a certain value).

2.4.1 Software environment to create image capture and processing tools

In this thesis image analysis tools available in the Openlab Automator (Perkin Elmer, USA) and in ImageJ have been used for image processing. ImageJ is a public domain image-processing program, originally developed by Wayne Rasband at NIH (<http://rsbweb.nih.gov/ij/docs/intro.html>). It is an experimental, Java-based system, where any user can share plugins and write their own macros designed to answer specific image processing questions. ImageJ is free and runs as an online applet or as a downloadable application on any computer. There are several other techniques/programs researcher can use to create custom-built algorithm for image processing. KNIME is, like Openlab Automator, a visible programming language allowing the researcher to design intuitive flowcharts that are able to perform complex image processing and analysis tasks without the need to write computer code (Quintavalle, Elia et al. 2011).

2.5 CANCER

Cancer is a global problem with an estimate of 12,7 million people diagnosed in 2008 (Figure 2.5). In the same year, 7,6 million cancer deaths occurred, which is equivalent to the loss of 14 lives per minute (Figure 2.6). 56% of the diagnosed cases and 63% of the cancer deaths occurred in the economically developing countries of the world (Ferlay, Shin et al. 2008; Ferlay, Shin et al. 2010). Worldwide, calculating with an average life expectancy of 68 years, one of eight persons will be diagnosed with cancer during their lifetime. In Western Europe, where life expectancy is 80 years and the incidence of cancer is high, one of three people will be affected by cancer during their life (Klein 2009; CancerResearchUK and IARC 2011). The world population is ageing: the global burden of cancer continues to increase largely because of the aging factor and growth of the world population, alongside with an increasing adoption of cancer-causing behaviors, particularly smoking, in economically developing countries (Jemal, Bray et al. 2011).

Cancer is not just one disease, approximately 200 different diagnoses are found in humans. The five most common cancer types in the world are, in order, lung, breast, colorectal, stomach and prostate cancer. Together they represent almost half the of all cancers cases; 48,3% or 6,1 million cases (Figure 2.5) (Ferlay, Shin et al. 2008).

2.5.1 Why do we get cancer?

Most cancers trace their origin to a single transformed cell. This single cell resides within a body of cells that are more numerous than there are stars in our galaxy (10^{11} stars in the Milky Way galaxy) (Morrison, Wolff et al. 1995). The human body is comprised of around 5-10 trillion (10^{13}) cells, which all share the same instructions inside their DNA code (Alberts, Johansson et al. 2002). In different organs, cells have specific sets of genes activated, which allow them to express a repertoire of proteins needed for the proper function of that organ. Cells are dependent on each other and on the surrounding environment for their survival. A

complex network of signalling orchestrates the activities within and the interplay between cells. Each day, 50 – 70 billion (10^9) cells die due to apoptosis in the average human adult (Chen and Lai 2009). To maintain homeostasis many cells will also have to go through division.

Cancer is a disease involving changes in the genome of cells and in the surrounding environment (Hanahan and Weinberg 2000; Bissell and Radisky 2001). At the single cell level cancer has been defined as the consequence of mutations that involves oncogenes with dominant gain of function and/or tumor suppressor genes with recessive loss of function. A normal cell evolves by multiple stepwise changes (tumor progression) to a neoplastic state (Foulds 1954). In order to progress to a tumor, the cell has to acquire certain capabilities, defined as the hallmarks of cancer. This multistep process of accumulated changes allows normal cells to become tumorigenic and ultimately metastatic (Hanahan and Weinberg 2000; Bozic, Antal et al. 2010).

The original six hallmarks of cancer development, as defined by Hanahan and Weinberg 2000, has as of 2011 been re-defined and accompanied by two more emerging hallmarks with potential generality (Hanahan and Weinberg 2011);

- 1) Sustaining proliferative signaling
- 2) Evading growth suppressors
- 3) Resisting cell death
- 4) Enabling replicative immortality
- 5) Inducing angiogenesis
- 6) Activating invasion and metastasis
- 7) Reprogramming energy metabolism
- 8) Evading immune destruction

A tumor is more than just millions of transformed cells. It is a heterogeneous and complex tissue, which can even be regarded as a new organ (Bissell and Radisky 2001; Mueller and Fusenig 2004; Bissell and Hines 2011). The interactive signalling between the tumor and the stroma contributes to the complexity of this tissue (Mueller and Fusenig 2004). Therefore, to understand the biology of tumors, it is essential to also look at the different types of (ostensibly) normal cells within or in the immediate vicinity of the tumor (the tumor stroma). On a “micro-macro” level, the acquired sets of functional capabilities result in the autonomous growth of a new tissue that has escaped normal restraints on cell proliferation and show varying degrees of fidelity to their precursors and to the original function of the organ (Rubin, Strayer et al. 2008). The understanding that the tumor microenvironment and tumor stroma is essential for tumorigenesis, has (after many years) now become consensus in the field (Hanahan and Weinberg 2011).

GLOBOCAN 2008 (IARC)

WORLD CANCER INCIDENCE

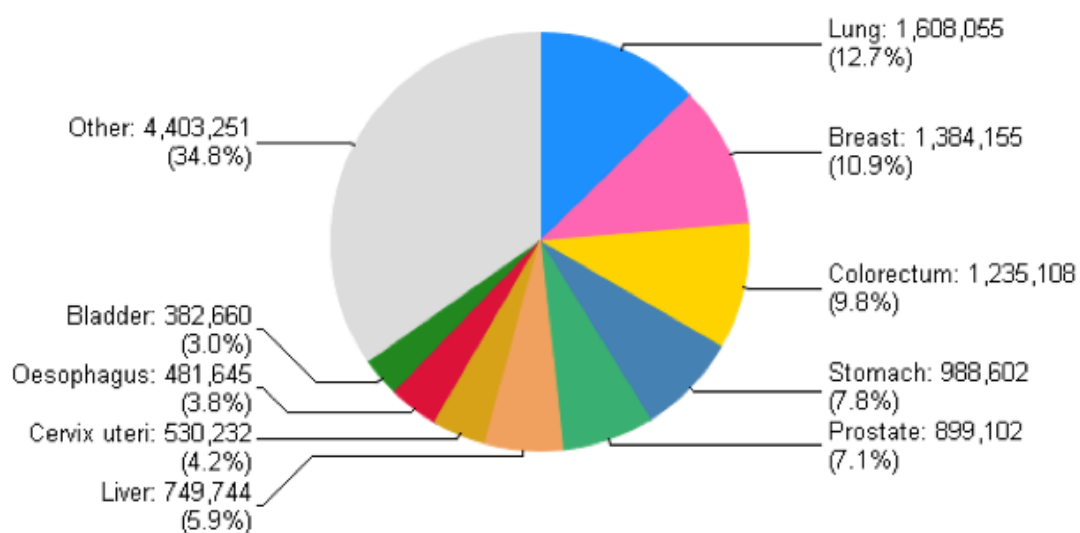


Figure 2.5 Estimated number of cancer cases 2008. World: both sexes, all ages (total: 12 662 554) Source: (Ferlay, Shin et al. 2008)

WORLD CANCER MORTALITY

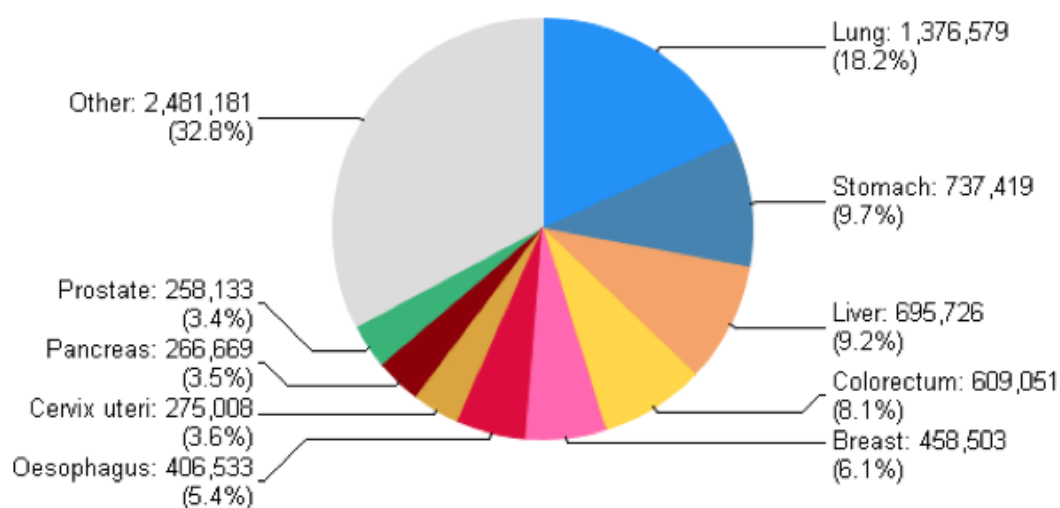


Figure 2.6 Estimated number of cancer deaths 2008. World: both sexes, all ages (total: 7 564 802). Source: (Ferlay, Shin et al. 2008)

2.5.2 Normal stroma versus tumor stroma

Genetically abnormal cells define the epithelial parenchyma of carcinomas, whereas recruited cells of mesenchymal origin constitute the tumor-associated stroma. The surrounding and interwoven stroma provides a connective-tissue framework for the tumor tissue. The stroma compartment includes many different cells, including fibroblasts, adipocytes, infiltrating immune cells and endothelial cells (Mueller and Fusenig 2004; Weinberg 2008).

Fibroblasts are the main cellular component of the connective tissue and they are found embedded in a fibrillar matrix. This matrix, or more correctly the extracellular matrix (ECM), is a complex three-dimensional network of macromolecular protein fibers and non-fibrous proteoglycans. The ECM is a multitasking unit as it provides architectural structure and strength as well as contextual information for cellular communication, adhesion and migration (Mueller and Fusenig 2004; Parsonage, Filer et al. 2005). Fibroblasts are responsible for the production of many components of the ECM, such as type I, III, V-collagens and fibronectin. They also contribute to the formation of the basement membrane by secreting type IV collagen and laminins (Woodley, Stanley et al. 1988; Chang, Chi et al. 2002). The laminins are large heterotrimeric glycoproteins that are major components of the extracellular matrix (Zagris, Chung et al. 2000). Fibroblasts are key players in the connective tissue not only because they synthesize its building blocks, but also because they are an important source of proteolytic enzymes such as the family of matrix metalloproteinases (MMPs). Through their production of such ECM-degrading proteases they also play a crucial role in maintaining ECM homeostasis by regulating ECM turnover (Kalluri and Zeisberg 2006). MMPs constitute a family of over 24 members, which collectively are capable of degrading virtually all protein components of the ECM (Lynch and Matrisian 2002).

For tissues to stay devoted to their function during development, adult tissue remodeling and tissue homeostasis depend upon the strict maintenance of a complex spatial and temporal dialogue between the epithelium and the cellular and acellular components of the tissue stroma (Weaver and Gilbert 2004). Cells communicate with each other and with the ECM dynamically, via junctions and receptors (such as the ECM receptor family of integrins) hormones and other soluble factors (Varner and Cheresch 1996; Bissell and Hines 2011). In addition, fibroblasts also secrete growth factors that direct mesenchymal-epithelial cell interactions (Kalluri and Zeisberg 2006).

In undisturbed adult tissues, fibrocytes are post-mitotic resting cells. As part of a regenerative response after tissue damage, fibrocytes become metabolically activated fibroblasts and re-enter the cell cycle. This process is primarily initiated by platelet-derived growth factors (PDGF) released from the aggregated thrombocytes at the site of injury. Activated fibroblasts are actively engaged in pro-inflammatory signaling and participate in the recruitment of immune-effector cells. Fibroblasts are responsible for the replacement of the temporary barrier of the wound (the clot) with a permanent scar tissue. Fibroblasts also communicate with the damaged epithelial compartment and participate in the regulation of re-epithelization through a complex signaling network that involves, amongst others, various members of the TGF- β family. At the later stage of wound healing response, fibroblasts can be converted to contractile myo-fibroblasts that are responsible for the contraction of the scar tissue.

In normal tissues, fibrocytes are not directly adjacent to the cells of the parenchyma. The basement membrane acts as a barrier separating the epithelium from the surrounding stroma, which plays an important role in tissue architecture and compartmentalization (Tanjore and Kalluri 2006). The integrity of the basement membrane also defines the

tumor microenvironment by providing significant host-derived regulatory signals during progression of tumor growth and metastasis (Tanjore and Kalluri 2006).

Cancer initiation, progression, and invasion occur in this complex and dynamic stroma microenvironment (Sautes-Fridman, Cherfils-Vicini et al. 2011). The tumor stroma contains various fibroblast-like cells of mesenchymal origin e.g. carcinoma-associated fibroblasts (CAFs), pericytes/mural cells and vascular smooth muscle cells (Ostman and Augsten 2009). CAFs show certain resemblance to contractile myo-fibroblasts. The separation of CAFs from normal cell is not a trivial task. Markers that are routinely used to identify CAFs, such as alpha-smooth muscle actin (α -SMA), platelet derived growth factor receptor beta (PDGFR β) and neuron-gial antigen-2 (NG2), overlap with each other in identifying a mixed population of fibroblasts (activated or resting), myofibroblasts, pericytes and vascular smooth muscle cells. The S100A4 protein/fibroblast specific protein-1 (FSP1) has been identified as a more suitable marker for CAFs (Sugimoto, Mundel et al. 2006). Recent data established a functional role for Hedgehog signaling, primarily in the tumor microenvironment, where it is involved in myofibroblast differentiation and the induction of stroma-derived growth promoting molecules. Since the protumorigenic functions of the abundant stromal desmoplasia is typically associated with pancreatic cancer, targeting the Hedgehog pathway might prove to be beneficial in the treatment of the disease (Lauth and Toftgard 2011).

During the metastatic process, cancer cells migrate through locally different microenvironments, including the interstitium, the blood vessel endothelium, the vascular system and the tissue at a secondary site. The ability to successfully complete this journey and advance towards the formation and growth of a secondary tumor is dependent, in part, on the physical interactions and mechanical forces between cancer cells and the microenvironment. The physical interactions between a cell and the ECM play a key role in allowing cells to migrate from a tumor to nearby blood vessels (Lemaire, Deleu et al. 2011; Wirtz, Konstantopoulos et al. 2011).

Both the wound healing process and tumor development involve migratory cell movements. Chemotaxis of both tumor cells and stromal cells is an essential component of tumor dissemination during progression and metastasis. In fact, chemotaxis is now considered to be a potential prognostic marker, a treatment end point and a target of therapeutic intervention in cancer (Roussos, Condeelis et al. 2011). Active migration of tumor cells may require distinct phenotypic changes that are associated with the loss of epithelial markers (dedifferentiation) and gain of mesenchymal markers (epithelial-mesenchymal transition – EMT). The EMT transition is a highly conserved cellular program that allows polarized, immotile epithelial cells to convert to motile cells with mesenchymal features. This cellular program has been observed to underlie many of the tissue remodeling events during embryonic development and more recently been associated with cancer invasion and metastasis (Yang and Weinberg 2008).

Tumors require vascularization to surpass a certain minimum size (neo-angiogenesis). Angiogenesis is one of the hallmarks of cancer. Angiogenesis however is rarely perfect in tumors. The imbalance of pro- and anti-angiogenic signaling within tumors often creates an abnormal vascular network that is characterized by dilated, tortuous, and hyperpermeable vessels. This mess of abnormalities also influences the microenvironment and might fuel tumor progression. Moreover, it also leads to a reduction in the efficacy of chemotherapy, radiotherapy, and immunotherapy. Pre-clinical studies have shown that anti-vascular endothelial growth factor (VEGF) therapy can lead to vascular normalization, with a reduction in hyperpermeability, increased vascular pericyte coverage and resulting in a more

normal basement membrane and this in combination with chemotherapy leads to improved clinical outcomes (Brown, Guidi et al. 1999; Goel, Duda et al. 2011).

2.5.3 Tumor microenvironmental control – why don't we all get cancer?

If one in three people will get cancer, why then will two of three not get cancer? What are the underlying mechanisms that protect the majority of us from cancer?

A large number of genes are now known to influence cancer development in a cell autonomous fashion. The illegitimate activation or inactivation of oncogenes and tumor suppressor genes, respectively, by genetic or epigenetic mechanisms is now a very well studied field. There are various ways to protect the integrity of the body against the emerging cancer. At least five types of surveillance functions have evolved to counteract the probability of cancer development (Klein, Imreh et al. 2007).

They can be classified as follows:

- immunological (mainly directed against virally induced tumors)
- genetic (DNA repair, checkpoint functions)
- epigenetic (imprinting, chromatin structure)
- intracellular (programmed cell death)
- intercellular (microenvironmental).

The microenvironmental control is emerging as a major restraining force that can prevent the growth of malignant cells (Klein, Imreh et al. 2007; Klein and Demant 2008; Klein 2009; Allen and Louise Jones 2011; Bissell and Hines 2011). It may be partially or fully responsible for Peto's paradox, the fact that large mammals do not have more tumors than small rodents, in spite of the high degree of conservation of oncogenes, tumor suppressor genes and signal transduction pathways that control cell proliferation (Bredberg 2009; Caulin and Maley 2011). Traditionally, this restraint has been attributed to immunological mechanisms. The role of the immune system in tumor development is complex, as shown by the many possible infiltrating immune cells in the tumor stroma. Solid tumor infiltration by immune cells can be both a good and bad prognostic marker (Zitvogel, Kepp et al. 2010). For example, macrophages may promote tumor growth by chronic inflammation whereas infiltrating T and NK cells may control cancer development (Pages, Galon et al. 2010). However, in many cases the immune system "tolerates" the tumor allowing it to survive. The control function of the immune system is evident in immunosuppressed individuals, where oncogenic virus infections often leads to tumor development, such as Kaposi sarcomas, diffuse large cell B-cell lymphoma, cervical and liver cancer (Schulz 2009; Vajdic and van Leeuwen 2009). Post-transplant lymphoproliferative disease, a malignant B-cell lymphoma caused by Epstein Barr virus (EBV), is an extreme example of an opportunistic tumor, which is only able to take over when the patients immune system is severely compromised (Bower 2002). It is clear that the immune system is involved in surveillance against tumors, but it is also becoming obvious that non-immune controls play a major role in the protection against non-viral tumors, regarded as "self" by the immune system. After all, these cancers constitute more than 80% of all tumors (Hanahan and Weinberg 2011).

In 1775, Percival Pott found an association between exposure to soot and a high incidence of squamous cell carcinoma of the scrotum in London's chimney sweeps. This was the first example of a specific cancer related to a specific occupation, demonstrating that a malignancy could be caused by an environmental carcinogen (JAMA 1963). In the early

1940's, Berenblum showed that the weakly carcinogenic croton oil, applied alternately with small doses of benzopyrene to mouse skin induced a larger number of tumors than benzopyrene would do alone. Subsequently, Moltram found that a single subcarcinogenic dose of benzopyrene followed by multiple applications of croton oil could induce a large number of skin tumors. These experiments provided the basis for the two stage model of carcinogenesis where the initiator (mutagen) agent has to be followed by a non-mutagen irritant to induce skin cancer with high likelihood (Slaga 1983). Chemical identification of different tumor promoters showed that their main action was to generate unspecific tissue damage, local inflammation and reactive hyperplasia in the near vicinity of the mutagenized cells. This points in the direction of the potential importance of the altered microenvironment in the course of tumorigenesis. Other early evidences, for the capacity of normal cells to inhibit cancer cells, came from Stoker in the 1960's showing that normal mouse fibroblasts can inhibit the growth of polyoma virus transformed hamster tumor cells (Stoker 1964; Stoker, Shearer et al. 1966)

The revolution in molecular biology, from 1953 and onwards, contributed to a strong focus on transformation associated genetic lesions in the tumor cells, as the cause of cancer. The role of a potential microenvironmental control of tumor growth was not sufficiently appreciated, despite the early findings suggesting its important role. The interest in the role of normal non-damaged tissue in the control of neoplasia was raised first after it was shown that reestablishment of normal tissue architecture can override the malignant phenotype. Rous sarcoma virus, carrying the very potent oncogene v-src, could not give rise to tumors when introduced into chick embryos but could massively transform the chick embryo cells when they were separated in culture. On the other hand, Rous sarcoma virus could induce tumors in association with wounds in the chick (Dolberg and Bissell 1984). This suggested that the context, the surrounding environment, in which the cells exist, determines their fate (Beliveau, Mott et al. 2010; Bissell and Hines 2011). A striking example of this can be highlighted by the experiments of Mintz and Illmensee who demonstrated that it was possible to normalize malignant mouse teratocarcinoma cells by implantation into early mouse embryos (Mintz and Illmensee 1975). Reconstruction of polarity and/or acinar structure in epithelial tumors or induction of differentiation in hematopoietic or germ cell derived tumors, are other examples that may prevent or reverse malignant growth (Itoh, Nelson et al. 2007; Partanen, Nieminen et al. 2007; Partanen, Nieminen et al. 2009). In contrast, disruption of the normal tissue equilibrium by inflammation, regeneration or wound healing may promote the growth of potentially or frankly neoplastic cells (Beliveau, Mott et al. 2010; Erez, Truitt et al. 2010).

2.6 DRUG SENSITIVITY ASSAYS

2.6.1 How can we find the best drug for one patient

Why is cancer in so many cases so difficult to cure? Part of the explanation may be the escape of tumor cells from multiple controls illustrated by the accumulation of several changes both within the tumor and within the tumor stroma. Moreover, cancer is a personal disease; every cancer is different as every person is different from each other. Most of the 200 different cancer diagnoses in humans can be further split into numerous prognostic subgroups, based on various histological and molecular progression markers (Wright, Tan et al. 2003; Barton and Swanton 2011; Schwalbe, Lindsey et al. 2011).

The clinical experience shows that patients, even with the same form of cancer, at a similar stage of disease, may respond differently to treatment. The greatest challenge of modern cancer therapy is to develop individualized treatment for each cancer patient.

Trying to treat most cancers means to expose the patients for heavy drug treatment in combination with radiation and surgery. The side effects of the treatment can be devastating and are often the major limiting factor of the therapy. In other words, cancer treatment involves considerable risks, pain and suffering for the patients (McKnight 2003). Caring for cancer patients belongs to the most expensive activities of the healthcare system (Karlsson, Nygren et al. 2001). Cancer drug treatment protocols are the result of carefully controlled clinical trials involving thousands of patients over many years. During the last decades we have seen a striking improvement in patient survival in several forms of human malignancies, particularly in leukemias and lymphomas. The development was the most impressive in the case of pediatric leukemias (Terracini, Coebergh et al. 2001). For these diseases the careful grouping of patients according different biological markers and prognostic indicators proved to be crucial for selection of the most effective treatment protocols. These protocols heavily rely on the use of relatively old drugs that were developed in the late 1960's and early 1970's. Key factor to achieve the greatly improved survival was the rigorous adherence to highly standardized treatment protocols. This strategy, although very successful in terms of saving lives of pediatric patients, resulted in very aggressive treatment with significant toxicity. Moreover this strategy left very little room for introduction of novel drugs (Ablett, Doz et al. 2004).

Today there are more than hundred anticancer drugs approved in the European Union. In addition there are several hundred new drugs in clinical trials or in the development pipeline of the pharmaceutical industry. It is notable that it is only 68 years ago since a Hodgkin's lymphoma patient was the first cancer patient to be treated with chemotherapy (Hirsch 2006; Joensuu 2008). The plethora of different possible effective drugs today leads to a logistically very difficult but important challenge: how to find the most suitable drug for any given patient (McKnight 2003).

There are different ways to approach individualized therapy in the cancer ward. One way is to try to generate an extensive molecular map of the tumor with the expectation that this will lead to better understanding of the behavior of the tumor and consequently to more efficient therapy. The precise molecular mechanism of many cancer associated regulatory changes has been elucidated and led to the treatment of "druggable targets" in cancer (Hsieh and Moasser 2007; Perrotti and Neviani 2008).

Another way is to use *in vitro* drug sensitivity assays to determine the sensitivity profile of tumor cells. This approach was already introduced forty years ago to analyze leukemic cells (Bertelsen, Sondak et al. 1984). A variety of techniques were developed that aimed to determine the viability of tumor cells after *in vitro* culturing with the relevant drugs. Some of these techniques are widely used such as the ATP conversion, MTT-reduction or FMCA (fluorometric microculture cytotoxicity assay) assays and were proven to be able to provide clinically useful information about the drug sensitivity of cancer cells (Larsson and Nygren 1993; Larsson and Nygren 1993; Nygren, Fridborg et al. 1994; Hayon, Dvilansky et al. 2003; Sargent 2003).

The potential of high-content high-throughput microscopy assays in drug discovery has previously been demonstrated (Starkuviene and Pepperkok 2007). To use automated high throughput imaging to measure the effect of different drugs on cell viability is a commonly applied industry scale technique, regularly used by all the major pharmaceutical companies for large-scale drug screening projects. Only selected academic institutions or consortia can afford to operate these devices in basic research. Furthermore, high throughput imaging devices are practically absent from routine clinical laboratories.

In this thesis we have developed an automated drug sensitivity microscopy assay (viability assay). Using automated fluorescence microscopy and robot printed drug plates we can measure drug effects, at the single cell level, of many different drugs in a parallel fashion.

Examples of results from drug sensitivity tests:

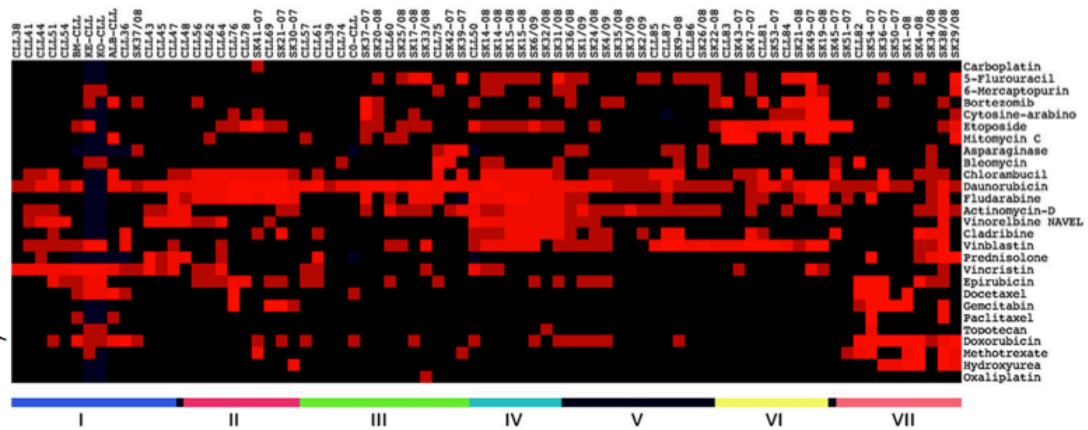


Figure 2.7 Hierarchical clustering of *in vitro* drug sensitivity data of 77 primary CLL samples. The intensity of the red color corresponds to drug sensitivity. Seven-patient subgroups were identified on the basis of co-segregating drug-sensitivity patterns and are marked with Latin numerals. Figure adapted from (Skribek, Otvos et al. 2010).

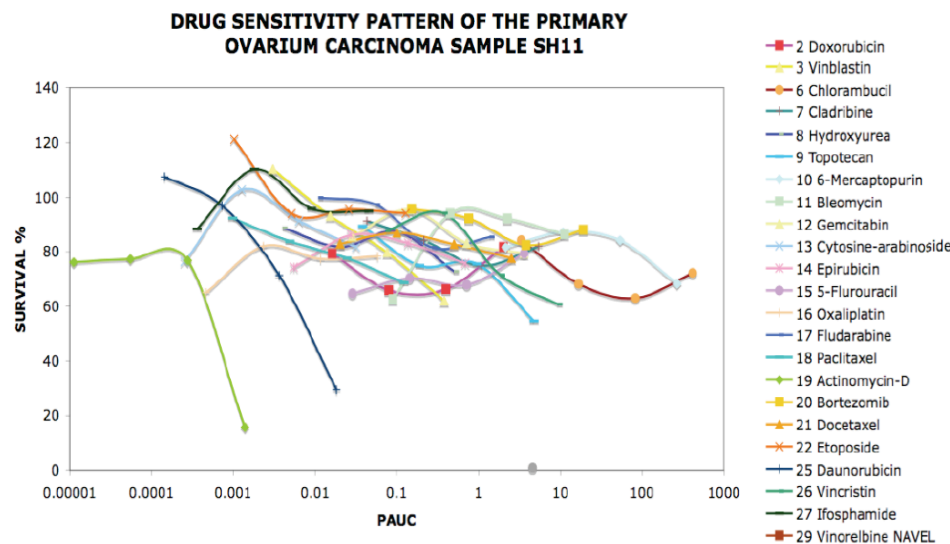


Figure 2.8 Illustrating the need for individualized cancer therapy. It may be possible to find drugs that are effective to very resistant tumors. Even though the tumor cells from a late stage ovarium cancer were found to be resistant for the majority of the drugs tested, two drugs showed concentration dependent effects (Markasz et al, unpublished).

3. RESULTS AND DISCUSSION

MICROSCOPY SYSTEMS

Automated platform 1 (Paper I - IV):

Confocal + widefield

Modified UltraVIEW LCI (Perkin Elmer, USA)
Zeiss Axiovert 200 M, inverted (Zeiss GmbH, Göttingen, Germany)
CSU10 Yokogawa spinning disc confocal unit (Yokogawa, Japan)
Motorized XY-table (Märzhauser, Germany)
ORCA ER cold CCD camera (1344×1024 px) (Hamamatsu, Japan)
Illumination:
Argon-Krypton Laser; 488 nm, 568 nm, 647 nm (Melles Griot, USA)
Mercury lamp (Osram); 365 nm
Mac OS X (processor Dual 2.5 GHz PowerPC G5)
RAM memory 2GB

Automated platform 2 (Paper VI; Extended field movie):

Confocal + widefield

Modified UltraVIEW LCI (Perkin Elmer, USA)
Zeiss Axiovert 200 M, inverted (Zeiss GmbH, Göttingen, Germany)
CSU10 Yokogawa spinning disc confocal unit (Yokogawa, Japan)
Motorized XY-table (Märzhauser, Germany)
ORCA ER cold CCD camera (1344×1024 px) (Hamamatsu, Japan)
Illumination:
Solid state laser 491 nm & 561 nm (Cobolt, Sweden)
Mercury lamp (Osram); 365 nm
Mac OS X (processor Dual 2.5 GHz PowerPC G5)
RAM memory 2GB

Automated platform 3 (Paper V - VI):

Widefield

Nikon Diaphot 200, inverted (Nikon, Japan)
Motorized XY-table (Märzhauser, Germany)
Illumination:
X-Cite 120 (Lumen dynamics, Canada)
Retiga-4000RV (2048×2048 px) (QImaging, Canada)
Mac OS X (processor 2 x 3 GHz Quad-Core Intel Xeon)
RAM memory 8GB

3.1 PAPER I

Extended Field Laser Confocal Microscopy (EFLCM): Combining automated Gigapixel image capture with in silico virtual microscopy

In Paper I, we demonstrated that it was possible to create a high-resolution, seamless confocal Gigapixel-montage (5,75 mm x 4,98 mm area) by combining automated image capture with Nipkow spinning disk confocal microscopy (Figure 8, Paper I). We have developed a set of computer programs that controls automated image capture (Quantcapture 4.0, Figure 1, Paper I) and seamless stitching of large image stacks (the Virtual Microscopy program, Figure 2-6, Paper I). We also showed that this method allowed extended field imaging, in confocal or wide-field mode at low or high resolution, of full mount embryos (Figure 3.1.1) and of transfected cells on culture slides (Figure 3.1.2).

Performing automated confocal fluorescence microscopy over large areas at high magnification and high-resolution, imposes several requirements on the capture process. The narrow field of view of high magnification objectives requires the capture of many consecutive tiles in order to span large xy-dimensions. The reduced depth of field of high-resolution optics let only a thin layer of the sample to be in focus at one time, which requires the capture of several z-planes to ensure that the entire volume of a specimen is included (Farkas, Leif et al. 1999; Hammond and Glick 2000). In addition, neither the xy-stage of a microscope, microscope slides nor mounted specimens are completely horizontal and no z-motor works without a z-drift. A major challenge in multi-field captures is therefore to find and to keep the object in focus across an extensive stage travel. Different methods of auto-focusing processes include reflection of reference points or the illumination of the specimen to find the optimal focus (Bravo-Zanoguera, Laris et al. 2007). These processes demand extra modules, are relative time consuming and most importantly they exhibit the sample for additional illumination with potential photobleaching and phototoxic effect, without generating any additional information.

Using single-point scanning confocal (SPSC) system the total capture time depends on the time needed to scan each focal plane. To reduce the scanning time by increasing the intensity of the laser illumination will only work to an upper limit defined by fluorescence saturation. Too intense excitation will deplete the electronic ground state of the fluorophore, and instead of the desired effect, effectively decrease the fluorescence and increase phototoxicity (Wang, Babbey et al. 2005). The collection of multi-field images with individual optical sections will also require extensive memory handling capacity and complicated 3D-rendering software for volume stitching.

In order to reduce the scanning time and increase the sensitivity of the detector system, we chose to use cold CCD camera combined with the Yokogawa spinning disc confocal unit to minimize out-of-focus blur. Our aim was to collect all signals through the z-depth of the specimen, without rendering a 3D volume.

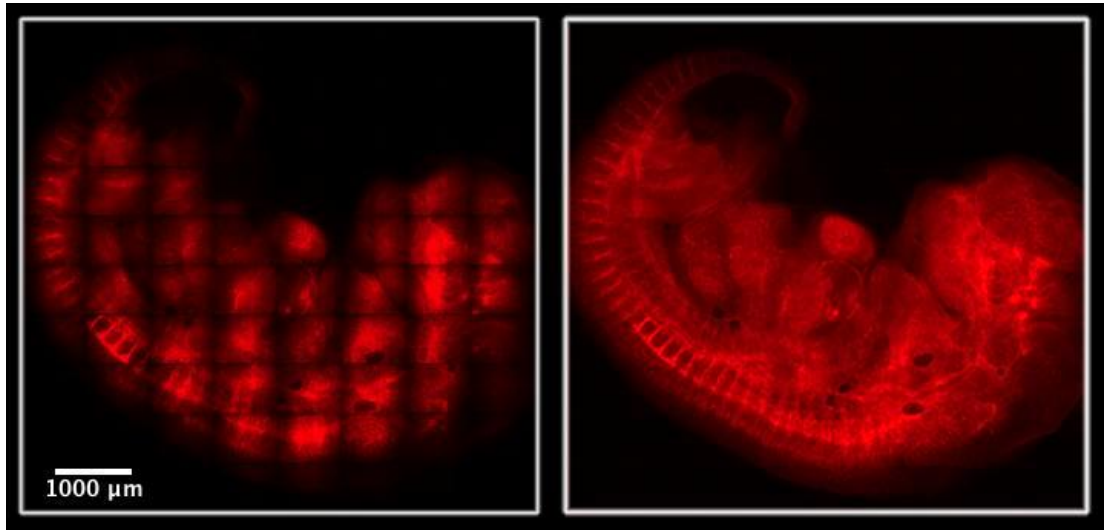


Figure 3.1.1 Extended field microscopy of whole mount embryo, visualizing blood vessels using endothelial CD31 antibody-staining (staining by Renhai Cao, with kind permission to reprint) 10 x 8 fields, 10X; (835 x 636 μm /field). Raw images (left), after flat-fielding and pixel precise alignment image processing (right). Figure modified from (Zhou, Tian et al. 2007).

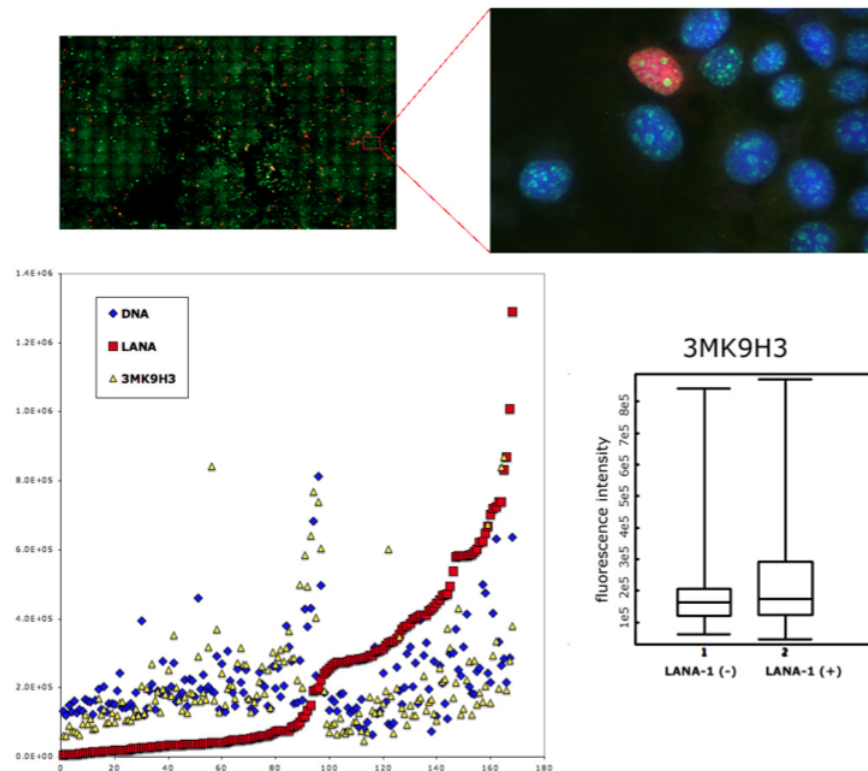


Figure 3.1.2 LANA-1 expression does not affect 3MK9H3 (green) levels as measured using extended field laser confocal microscopy (EFLCM), 300 (20 x 15) adjacent fields (as illustrated by the mosaic image and zoom-in at individual nuclei image). The total fluorescence intensity measurement for 3MK9H3, DNA (blue) and LANA-1 (red) of individual nuclei, is plotted in the order of increasing amount of LANA-1 (Y-axis: fluorescence intensity, X-axis: number of cells). The amount of 3MK9H3 staining is also compared on population levels of LANA-1 positive and negative nuclei on a box chart. Reprint from (Stuber, Mattsson et al. 2007).

The Quantcapture 4.0 program was developed using the visual programming language Openlab Automator. The visual programming environment allowed us to design flow-charts of icons linked together to control each step of the image capture process. In addition to the hardware control, the language also maintains image processing and measurements tools supporting the declaration of string, numeric and array variables (bird-eye view of the flowchart, illustrating the concept, can be found in Figure 1, Paper 1 and under Methodological considerations, Figure 6.2.3 A).

In Quantcapture 4.0, the first command prompts the user to define the extent of the capture area, by fixed numbers of images in the xy-direction or by a manual selection of xy-coordinates. The user defines the z-values for the highest and lowest focal planes, at each corner of the capture area. The z-depth is calculated as the difference between the extremes of the 8 different z-values, ensuring that the sample will be in focus during the extended field capture.

CCD cameras convert incoming photons into electrons that are stored in wells of a camera chip. A pixel-well value is read out as a voltage, which after amplification, passes through an analog to digital converter and forms an image of digital pixel values. Digital fluorescence images are always corrupted by different sources of noise (dark current, pixel non-uniformity, shot noise, etc.) that are introduced during the integration and read out of an image from a CCD. One problem with projecting an image stack is that noise from all of the optical sections is incorporated into the projection. This effect is particularly severe with sum intensity projections, where all value of each image is included, regardless if it is a true signal or noise. Capturing images at very low light level will increase the risk that also random pixel noise will be included in the final image even when using max intensity projection (Hammond and Glick 2000). This effect can be attenuated by use of median filtering.

Instead of capture single z-layers, we developed the Moving Z-capture process. This process let the sample move from top to bottom focus along the z-axis, while the cold CCD-camera collects all signals during one total exposure, without closing shutter in between the z-steps. Using the Moving Z-capture, only one image consisting of all signals along the entire z-axis is produced. The Nipkow spinning disc technique assures that only light with minimal out-of-focus blur reach the detector, from every focus plane. The z-travel was performed step-wise in both Moving Z-capture and in the conventional capture process. The exposure time at each step through the z-stack was identical between the two types of capture techniques. The difference was that in the Moving Z-capture the camera also collected signals even in between the steps, making the exposure time through the part of the z-depth that actually displayed the sample relatively longer compared to a single layer capture. Moreover, a sum-projection of individually captured z-layers multiplies the background camera noise by the number of z-layers. As we have measured, the background cold CCD camera noise contributes only once to the final image generated by the Moving-Z capture. This background was also removed using the total exposure "dark background" image (more technical details on the Moving Z-capture loop can be found under Methodological considerations, Chapter 6.2)

Images captured by the Moving Z-capture technique had better quality than images captured by a conventional confocal capture process (sequential capturing of z-planes). We compared images acquired using the Moving Z-capture (Figure 3.1.3 A) with 20 images taken from the identical z-depth but in a sequential fashion (Figure 3.1.3 C & 3.1.3 D). Figure 3.1.3 C & 3.1.3 D show the sum and maximum projections, respectively, of the 20 images-stack. Figure 3.1.3 B shows the quality of one single z-layer from the 20-images stack.

Comparison of the gray levels histogram for the different images show that the gray levels were more spread when the Moving Z-capture was performed, suggesting better contrast (Ramirez, Ozawa et al. 2011).

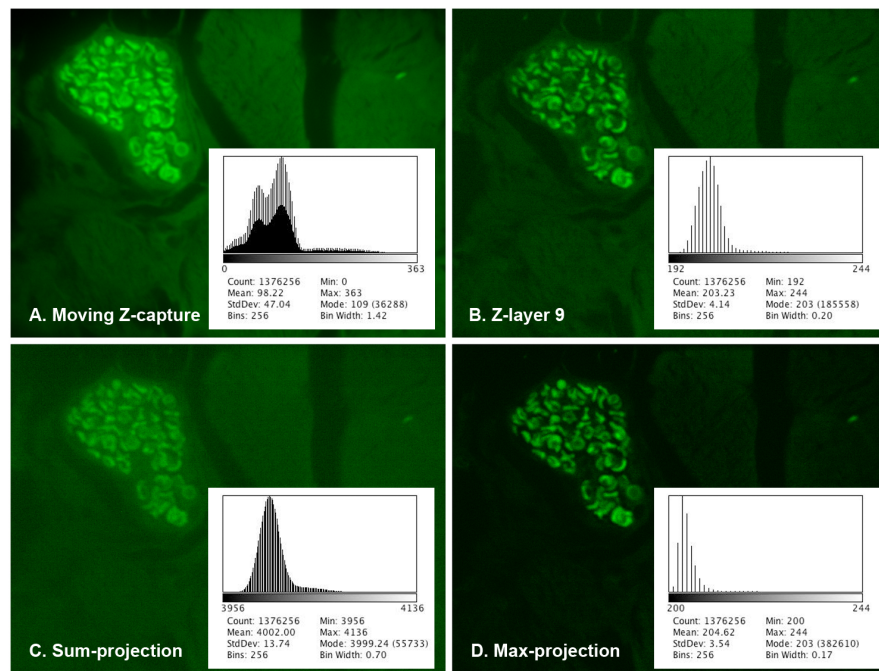


Figure 3.1.3 Moving Z-capture (A) versus single layer capture of 20 z-layers (B-D), z-layer in a stack of 20 images (B) sum-projections of 20 z-layers (C) max-projections of 20 z-layers (D).

In order to perform pixel precise alignment of 3000 confocal images into a seamless mosaic, every image was taken with a fixed overlap (Figure 4, Paper I). We introduced a new software for image processing; the ImageLab/Virtual Microscope program. Using this program, we could perform image processing and compensate for optical and mechanical imperfections, inherent in the automated image capture processes (due to motorized xy-step limitations, uneven illumination and misaligned camera) (Figure 5-6, Paper I). This software permitted image processing of large image data sets on ordinary desktop computers, commonly used in the academic environment, and allowed virtual microscopy visualization (Figure 2-3, Paper I).

Through this publication, we would like to advocate that visual programming languages enable users to make complicated but flexible image capture applications for automated microscopy, without broad knowledge of complex computer languages. The automated capture process allows image capture without a human bias in the selection (after initial settings) and it assures identical exposure times for all images. In summary, this technique allows quantitative measurements of (even weak) fluorescence signals and morphological parameters on a large number of cells or on entire histological sections.

The presented method, in combination with quantification programs developed by us in Openlab automator (QuantCount 3.0 and CytotoxCuant 3.0) was applied in different biological studies, such as imaging and quantification of epigenetic effects of transformation associated viral nuclear antigens, as shown in Figure 3.1.2 (Stuber, Mattsson et al. 2007) and quantification and analysis of labelled tumor cells in 384-well plates (Markasz, Kis et al. 2007; Markasz, Skribek et al. 2008; Markasz, Vanherberghen et al. 2008).

3.2 PAPER II

Multi-dimensional laser confocal microscopy on live cells in submicroliter volumes using glass capillaries

With the advancement of different cell separation techniques (multicolour preparative flow cytometry, combined positive and negative magnetic separation, direct micromanipulation of living cells etc.) there is an increasing need to study isolated rare cells in various biological context such as cell-cell communication and target-effector interactions, and to do this in limited volumes. In Paper II, we have developed a technology that permits live cell imaging of a very small number of cells at the maximal resolution of the light microscope, in multiple dimensions over time (Figure 7, Paper II).

In our experience, when incubating cells in a rich (high amino acid, high pyruvate) HEPES buffered medium with free radical scavenger selenium (Iscoves modified Dulbeccos medium) the cells were stable and performed normal functions unhindered when observed for many hours - days, in closed POCmini chambers, in 400-600 μ l incubation volumes (Perfusion-Open-Closed-system) (Figure 2.3). These observations prompted us to test much lower incubation volumes, for closed chamber live cell imaging.

We hypothesized that the round geometry of the thin walls of polymerase chain reaction (PCR) capillaries, at high magnification could be regarded as a sufficiently flat surface as not to distort the quality of microscopy images.

We demonstrated that living cells could be imaged in submicroliter volumes in glass capillaries using Nipkow disc based confocal microscopy (Figure 2-6, Paper II). We reasoned that using immersion oil with the same refractory index as the glass wall of the capillary the geometry of the wall does not necessarily have to be plane parallel. We tested two types of glass capillary set ups, one with 2-4 μ l volumes and one with submicroliter incubation volumes. In both cases we used 10 μ l glass capillaries designed for capillary PCR. These capillaries are particularly amenable for creating optically homogeneous thin capillaries upon heating and constant power pulling. The capillaries were loaded with cell suspensions using surface tension as the only source of power. A small drop of cells in culture medium, put on the hydrophobic surface of parafilm, could be fully loaded simply by touching it with the orifice of the capillary. Sealing both ends of the capillary created a closed and well-controlled environment that could support the life of the encased cells for hours. We found that this simple set-up gave comparable results to those complex, very expensive and cumbersome environmental chambers (with controlled CO₂, humidity and temperature) that are routinely recommended for live cell imaging experiments (Stephens and Allan 2003). The only technical requirement of our set-up is an objective heater that maintains the correct temperature of the immersion oil drop. Our set-up permits the adaptation of complex live cell experiments in any laboratory that posses an inverted fluorescence microscope with CCD camera and an objective heater. Additionally, a spinning disc system allow fast, confocal multidimensional imaging of the sample, with a low rate of photobleaching (Wang, Babbey et al. 2005).

3.3 PAPER III

Cytotoxic drug sensitivity of Epstein-Barr virus transformed lymphoblastoid B-cells - Drug sensitivity test using automated microscopy

Treating patients with Epstein Barr virus (EBV) induced B-cell lymphoma is a challenge. Patients who succumb to this disease are immunocompromised, a risk group that is already extra vulnerable for cytostatic drug treatment and its heavy side effects. Yet, this is in severe cases where the lymphoma is resistant to Rituximab (anti-CD 20 mAb) a necessary choice of treatment. Trying to find the most effective drug or drugs that would kill EBV-immortalized B-cells, at low concentrations, to minimize side effects, was the aim of this study.

EBV is one of the most common viruses in the human population. Normally the infection occurs asymptotically during childhood, while primary infection in adults leads to infectious mononucleosis in half of the cases (Lewin, Aman et al. 1987). Up to 90% of the adult population carries the virus, as a latent infection throughout life (Fields, Knipe et al. 1996; Kieff and Rickinson 2007). Latently infected B-lymphocytes are kept in check by cytotoxic T-lymphocytes, which exert a strong specific immunity (Rickinson, Lee et al. 1996; Gustafsson, Levitsky et al. 2000). When the immune system is suppressed, as it is in AIDS patients or due to medication in patients after organ transplantation, EBV may become lethal. Two forms of acquired immunodeficiency have dominated the last quarter of the twentieth century and are responsible for the majority of lymphomas in the immunosuppressed: post-transplantation lymphoproliferative disorders (PTLD) and AIDS-related lymphomas (ARL) (Bower 2002). The reported overall mortality for PTLD often exceeds 50% (Opelz and Dohler 2004). The prognosis for PTLDs occurring after bone marrow transplantation is even worse (Orazi, Hromas et al. 1997). EBV infects the B-cell, hijacks its genetic machinery and encodes transformation-associated proteins that drive the B-cells into massive proliferation, both *in vivo* and *in vitro*. The *in vitro* generated lymphoblastoid B-cell lines (LCL) show very similar properties to the *in vivo* disease and are therefore a good model for studying the clinical syndrome (Rowe, Young et al. 1991).

Using our automated fluorescence microscopy system 1, in combination with a fluid dispenser robot for drug printing, we have developed an assay for high throughput drug sensitivity testing. We have in Paper III studied the effect of 29 different drugs on 17 different lymphoblastic cell lines.

Summarizing the drug effect of all 17 LCLs and plotting the mean cell survival for each drug allowed us to identify potent cytostatic drugs against LCLs. We found four drugs that were highly effective, even at lower concentration than would be normally used in the clinic: vincristine, paclitaxel, methotrexate and epirubicin (Figure 4, Paper III).

Vincristine and methotrexate are already included in the treatment of PTLD. Epirubicin and paclitaxel on the other hand were not found in protocols for EBV induced lymphoproliferative diseases. Our data suggests that these two drugs, which are already accepted for use with well-known efficacy on other tumors, might be possible alternative treatments for PTLD.

The drug sensitivity assay was designed as a three-day long co-culture of cells and drugs in 384-well plates. The result was based on fluorescence showing the viability of single cells

after treatment, in comparison to untreated cells. Each drug was tested at four different concentrations, in triplicates, in a total pattern of 12 wells per drug (Figure 3.3.1). It is possible to measure the concentration dependent effect of 30 different drugs in one plate. The drug plates were produced using a fluid-handling robot. The dilution series and loading of a drug master-plate was fully automated. The master-plate then served as a template to mass-produce replica plates using metal pin printing technology.

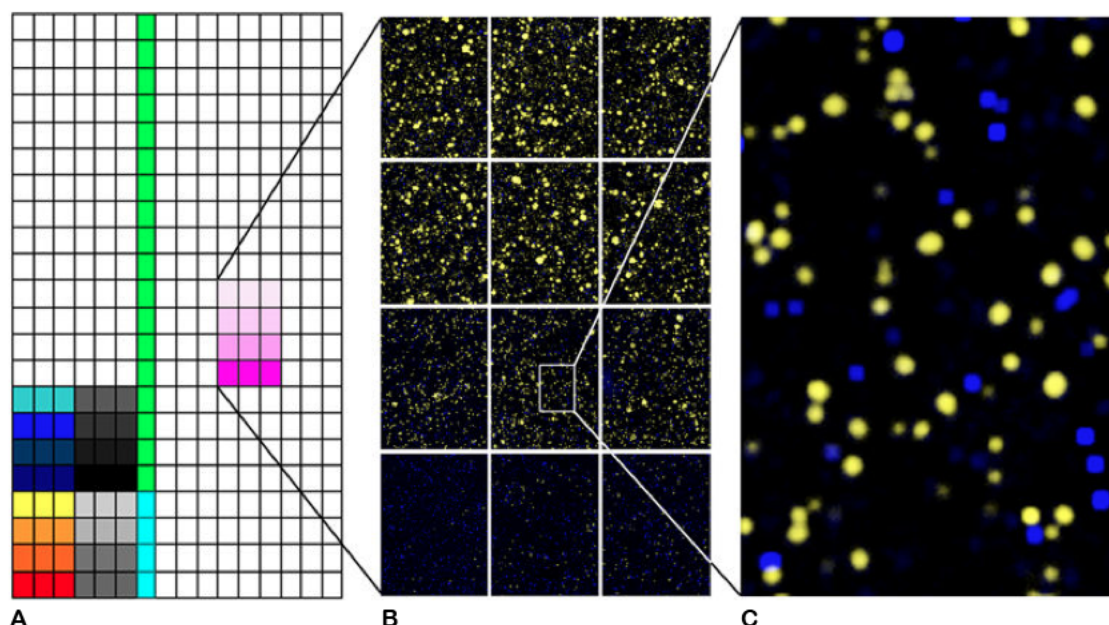


Figure 3.3.1 Drug dilution schedule in a 384-well plate. Each drug is tested in 4 concentrations and in triplicates (A). Concentration dependent drug effect: most cells are dead in the highest concentration of the drug (bottom panel) while most cells are alive in lowest drug concentration (top panel) (B). Live (yellow)/dead (blue) cell discrimination (C). Figure adapted from (Otvos, Skribek et al. 2011).

After three days of co-culture, a fluorescence dye mixture that discriminate between live and dead cells (VitalDye) was added to the cells. Two images per well (768 images per plate) were captured using the automated microscope platform 1. The extended field program QuantCapture 4.0, described in Paper I, was adjusted to fit for 384-well capture. The z-depth was calculated as the difference between the focuses in the four corner-wells and the Moving Z-capture loop was applied to ensure that all signals from cells at different z-levels were recorded during the xy-travel across the plate. Images were captured using low magnification (3.5 X) objective, allowing visualization of almost the entire well in one image. The Moving Z-capture proved useful, despite the non-optimized confocal settings at 3.5X. In our experience the laser excitation through the Yokogawa head (the Nipkow spinning disc confocal unit) gave better image quality than normal wide-field mercury lamp excitation.

Automatic quantification of all cells was performed using the program QuantCount 3.0, also developed by us in the visual programming environment Openlab Automator. Combining several image processing concepts into a single complex flowcharts made it possible to identify and count individual cells (bird-eye view of the flowchart, illustrating the concept, can be found under Methodological considerations, Figure 6.2.3 B) In essence, the background noise was calculated from four empty wells using a smoothing filter and was subtracted from the image stack. The smoothed background image was also used to map the illumination inhomogeneity across the area of the well. Using this pattern, a series of correction values were calculated corresponding to defined areas of ring shaped segments of isoluminescent fields. These values were used to multiply all the other images using the areas of the ring segments as binary masks. This procedure compensated for the inherent loss of fluorescence at the periphery of the wells.

A sharpening filter was applied to enhance the contours of the cells. An optional quality check for binary thresholding was also implemented that allowed direct visual interpretation of any selected image. This method permitted an easy adaptation of automated image quantitation for plates of variable background and fluorescence intensity. Objects were defined as pixel clusters over a defined cut-off intensity value and were represented by a binary mask. Quantification was done on objects larger than a pre-set pixel number matching the actual cell size, to exclude debris. The final analysis of cell numbers was performed in Excel. We developed sheets, linked in several layers in order to automatically calculate the number of living and dead cells. In Paper III, the data is presented as the mean cell survival of 17 LCLs together with standard deviation, marked with grey shadow (Figure 1-2, Paper III).

EBV transformed B-cells show little genetic heterogeneity due to the fact that the virus encoded latency associated proteins are solely responsible for the transformation. This fact was revealed in the uniform pattern of drug sensitivity among the lines tested. This uniform response in the measurements also served as a demonstration of the robustness and reproducibility of the assay.

The presented work pioneered our studies on drug sensitivity testing which we have carried out using the automated microscopy systems, over the last five years. The long-term goal with the presented method is to develop a high throughput optical assay for routine clinical use to determine the cytotoxic drug sensitivity of human tumor cells against all available licensed and experimental drugs.

3.4 PAPER IV

Effect of frequently used chemotherapeutic drugs on cytotoxic activity of human natural killer cells - Drug sensitivity test using automated microscopy and differential imaging

The aim of this study was to determine whether cytostatic drugs could interfere with natural killer (NK) cells mediated cytotoxicity.

NK cells are part of the innate immune system and they can have direct cytotoxic effect against tumor -and virus-infected cells (Cerwenka and Lanier 2001) (Figure 1, Paper IV). Elevated infiltration of NK cells into solid tumors is associated with better clinical prognosis (Coca, Perez-Piqueras et al. 1997; Ishigami, Natsugoe et al. 2000). For this reason they have become of great interest for the treatment of cancer. In immune-based adjuvant therapy settings, NK cells are administered in order to target malignant cells, with the hope of a better clinical outcome for the patient (Ruggeri, Mancusi et al. 2006). Drug sensitivity profiles of NK cell activity would be valuable information in NK cell based immunotherapy protocols. Previous studies have only assessed a few drugs for their effect on NK-cytotoxicity (Utsugi, Demuth et al. 1989; Ujhazy and Babusikova 1991).

In Paper IV, we measured the efficacy of NK cell mediated cytotoxicity after treatment of 29 different drugs, which are routinely used in the clinic to treat cancer patients. Our data implied that chemotherapy protocols including proteasome inhibitors (such as bortezomib) or anti-microtubule drugs (paclitaxel, docetaxel and vinblastine) may interfere with NK cell-based immunotherapy, if applied simultaneously (Figure 4A, Paper IV). It is well-known that microtubule-disrupting agents prevent the NK-mediated killing of target cells (Katz, Zaytoun

et al. 1982). On the other hand, we found drugs that had almost no inhibitory effect on NK cell-mediated killing, even at high concentrations. We therefore suggest that these: asparaginase, bevacizumab, bleomycin, doxorubicin, epirubicin, etoposide, 5-fluorouracil, hydroxyurea, streptozocin, and 6-mercaptopurine and could effectively be combined with adjuvant NK cell-based immunotherapy (Figure 4C, Paper IV).

The importance of cytostatic drug effects on NK cell activity is further underscored by our subsequent finding that efficient Rituximab treatment of EBV transformed B-cells requires preserved NK cell activity. We conclude that it is important to consider the choice of cytostatic drug treatment when it is administered in combination with monoclonal antibody therapy (Markasz, Vanherberghen et al. 2008).

In this study eight primary NK cell isolates were tested, all derived from healthy donor blood. The target tumor cell line was K562, a non-adherent, immortalized myelogenous leukemia cells line, known for its sensitiveness for NK cell killing activity (Lozzio and Lozzio 1979). NK cell isolates were treated with 29 different drugs, in four concentrations and in triplicates, in a 384-well plate set-up identical to the drug sensitivity assay described in Paper III. Instead of three days, NK cells were only co-incubated with the cytostatic drugs for 20 hours. K562-cells were labelled with a green fluorescent dye (compatible with living cells) and subsequently co-incubated with the drug-treated NK cells for 5 hours, in an effector-to-target ratio 6:1. We found that a 5-hour co-incubation was long enough to record NK cell mediated killing, which usually happens within the first hour (Figure 1, Paper IV). At the end of the incubation time, ethidium bromide was added to all wells, to selectively stain dead cells red. The automated microscope platform 1 and the QuantCapture 4.0 program, described in Paper I & Paper III were used to automatically capture images of all wells in the 384-well plate. The QuantCount 3.0 program (described in Paper III) was used to automatically quantify green (K562) and red (dead K562 and NK) cells. In this study the number of dead target cells defined the measure of NK cell killing efficacy, after drug treatment. Dead target cells were defined as the green labelled K562 cells that also were stained red. NK cells in culture can go through spontaneous apoptosis. This has to be taken into account when performing the dead cell quantification, since dead NK cells would also be stained red by the ethidium bromide. In order to only quantify dead target cells, we developed the CytotoxCount 3.0 image analysis program (bird-eye view of the flowchart, illustrating the concept, can be found under Methodological considerations, Figure 6.2.3 C). Using the visual programming environment in Openlab Automator we designed a program dedicated to the analysis of differential labelling of the same cells, in a mixed cell culture. We used “Boolean AND” based image comparison for the final readout of dead target (red and green double positive) cells.

3.5 PAPER V

High-throughput live-cell imaging reveals differential inhibition of tumor cell proliferation by human fibroblasts

The tumor microenvironment plays a significant role in cancer development (Tlsty and Coussens 2006; Li, Fan et al. 2007; Goetz, Minguet et al. 2011). It is now well known that the activated stroma, with recruited inflammatory cells and CAFs can promote tumor development (Ostman and Augsten 2009; Erez, Truitt et al. 2010). It is less well known what role the normal stroma has in the early stages of cancer. A growing body of evidence point toward a microenvironmental control function of the intact stroma, in regulating the

behavior of neoplastic cells (Dolberg and Bissell 1984; Glick and Yuspa 2005; Partanen, Nieminen et al. 2009; Beliveau, Mott et al. 2010). Whether there is any cancer relevant genetic variation in microenvironmental control of tumor development has not been studied at all. The mechanism of tumor microenvironmental control is only partly known, with all members of the ECM as potential effectors. Among its known effectors, fibroblasts occupy an important place. The ability of fibroblasts to inhibit tumor cell growth by direct contact, originally discovered by Michael Stoker in the 1960s, was our departure point in the work in Paper V (Stoker 1964; Stoker, Shearer et al. 1966).

The aim of Paper V was to compare the postulated inhibitory effect of a large panel of human primary fibroblasts (107 samples) on tumor cell proliferation. The primary fibroblasts were derived from skin of pediatric and adult donors and from hernia, nasal polyps and prostate (called internal) biopsies or surgical rest material from adult and pediatric donors.

Six tumor cell lines were included in the study: three prostate carcinoma lines LnCaP (lymph node metastasis), PC-3 (bone metastasis) and DU-145 (brain metastasis); two lung cancer lines, H1299 and A549; and one Epstein Barr virus (EBV) transformed lymphoblastoid cell line, IB4. The tumor cell lines were genetically modified to stably express EGFP or mRFP fluorescent proteins; cytoplasmic expression of EGFP (LnCap) or nuclear histone H2A expression of mRFP (PC3, DU145, H1299, A549 and IB4). The genetic labeling of tumor cells made it possible to follow the proliferation of single cells over time, without losing signal due to division (Figure 3.5.1).

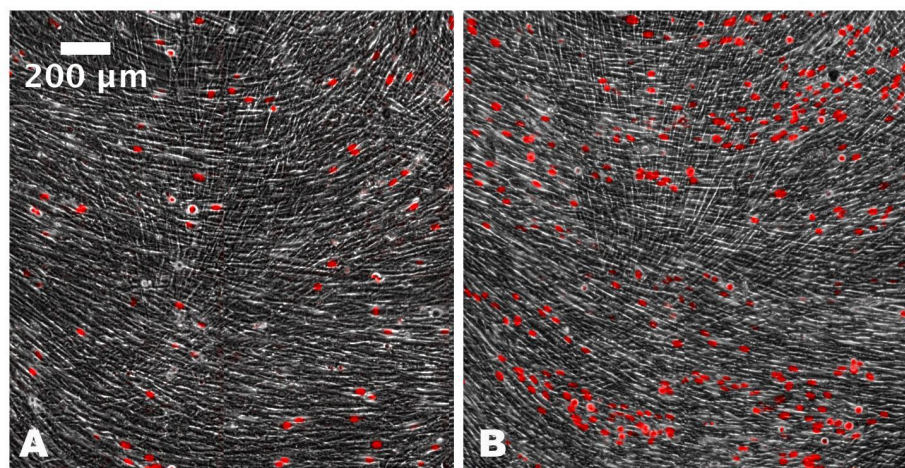


Figure 3.5.1. Illustration of the co-culture set-up: PC3mRFP tumor cells (red) growing on top of a confluent monolayer of pediatric hernia fibroblasts (phase contrast). Two time-points: day 0 (A) and day 3 (B).

The effect was investigated in a four-day long co-culture set-up, where color-labelled tumor cells were seeded on top of unlabelled fibroblasts. Fibroblasts from different donors were seeded into separate wells in a 384-well plate and were left for two days to form a confluent monolayer, before adding the tumor cells. The proliferation of tumor cells was recorded by images taken the same day as seeding (day 0) and after 4 days of co-culture with fibroblasts (day 4). Quantification at single cell level, of every tumor cell in all wells at each time-point, gave us the day 4/day 0 proliferation ratio for tumor cells growing on different fibroblast monolayers and in control wells (labelled tumor cells alone or labelled tumor cells together with unlabelled tumor cells). Fibroblasts were divided into subgroups dependent on their origin: adult skin, adult internal, pediatric skin and pediatric internal and were regarded as inhibitory if they, as a group inhibited tumor cell proliferation (Figure 3, Paper V).

We found that primary human fibroblasts differed in their capacity of inhibiting human tumor cell proliferation *in vitro*. The inhibitory effect depended on target tumor cell line, the donor age and the fibroblast site of origin. The majority of the fibroblasts could inhibit tumor cell proliferation (Figure 4, Paper V). The sensitivity to the inhibitory effect of fibroblasts differed between the six tumor lines. Four of six tumor cell lines (LnCap, DU-145, IB4 and H12999) were highly sensitive for fibroblast-mediated inhibition as demonstrated by the inhibitory effect of all fibroblasts as one group compared to the control (with a significant p-value <0,05) (Figure 3, Paper V).

Skin fibroblasts, of both adult and pediatric origin, were more effective in their inhibition of tumor cell proliferation than fibroblasts derived from internal sites (hernia, nasal polyp and prostate). Five of six tumor cell lines (LnCap, DU-145, IB4 and H12999 and PC3) were inhibited by all skin fibroblasts (as one group), with a significant p-value <0,05 (Figure 3, Paper V).

Sorting individual fibroblasts, according to their summarized inhibitory effect against all carcinoma lines, identified fibroblasts with consistently high and with consistently low inhibitory capacity. 9 of the 14 most inhibiting skin fibroblasts were derived from children. In the least inhibiting group, the majority of the fibroblasts were derived from internal sites and 11 of these 15 internal fibroblasts were derived from the prostate of adult donors (Figure 5 and 6, Paper V). All prostate biopsies were derived from prostatic cancer patients. There is a possibility that these samples could be cancer-associated fibroblasts. Conditioned media did not have any inhibitory effect on tumor cell proliferation, suggesting that the effect is contact mediated.

In addition, we could confirm the previously reported differential inhibition of SV40-transformed mouse 3T3 cells by isogenic non-transformed 3T3E and 3T3M fibroblasts, that had been characterized as strong and weak inhibitors, respectively (Figure 1, Paper V) (Allard, Stoker et al. 2003). We also found that the inhibitory effect of the 3T3 fibroblasts works across species barrier. Both the 3T3E and the 3T3M lines inhibited the proliferation all carcinoma cell lines (Figure 4, Paper V).

Using a 384-well plate, it was possible to analyze 12 different fibroblast samples against a panel of six tumor lines, in quadruplets, in one screening event. Fluorescently labeled tumor cells were co-cultured with fibroblasts and with unlabeled tumor cells as controls. Green (GFP labelled tumor cells) or red (mRFP labelled tumor cells) fluorescence images of all wells in the 384-well plate, were captured using automated fluorescence microscopy. Bright field images were captured to also register the unlabelled fibroblasts. The Quantcapture 4.0 program, developed in Paper 1 for automated extended field confocal microscopy, was modified for 384-well plate capture on a wide-field microscopy system (Platefocus 10 program, Microscope platform 3). Images were captured using low magnification (2.5 X) objective, allowing visualization of the entire well in one image. The depth of field (the range of the sample in focus along the optical axis) was relatively long (around 20 μ m) when using the 2.5X objective, often permitting acceptable focus control of across the 384-well plate (of the adherent cells on the bottom of the well), even without additional autofocusing. In the case of tilted plates, a brute autofocusing loop was implemented to find the best focus depth along a fixed number of z-steps. The stack of 384 images from each plate, mRFP labelled tumor nuclei or GFP labelled tumor cytoplasm, were quantified using image analysis tools in ImageJ.

We have found that performing background subtraction (rolling ball) followed by median filtering (3x3) in combination with the find maxima tool, was an effective way to automatically quantify tumor cells on single cell level (Figure 3.5.2 A-C). At low magnification

(2.5X), the mRFP-labelled nuclei appeared almost as point-like objects, suitable for find maxima identification. The stack of hundreds of images was automatically quantified by running the find FindStackMaxima macro in ImageJ. To quantify tumor cells labeled by cytoplasmic GFP, more considerations were needed. Background subtraction and median filtering was followed by a binary threshold and watershed segmentation, in order to separate adjacent cells from each other. When analyzing and quantifying the segmented cells, small debris could be excluded from the count by excluding particles smaller than a fixed number of pixels. This number was set to be significantly smaller than the average smallest cell. Quantification was performed using the Analyse particles plugin in ImageJ (Figure 3.5.2 D-F).

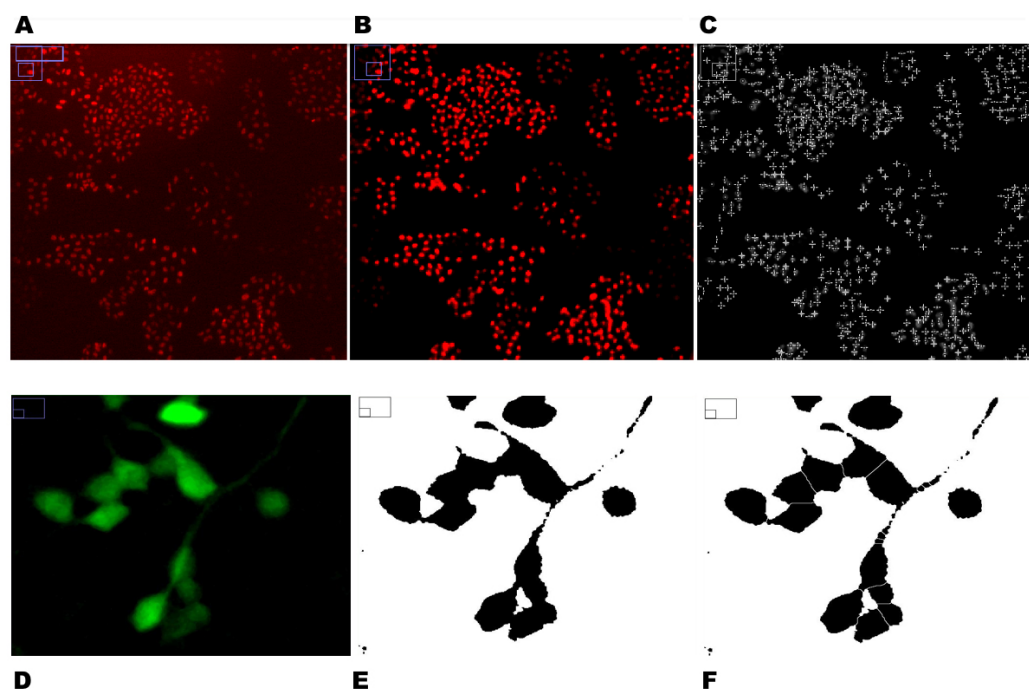


Figure 3.5.2 Image processing for automatic quantification of tumor cells. mRFP-H2A labeled tumor cells (2.5X): background subtraction (A), median filtering (B), find maxima identification of tumor cell nuclei (C). EGFP-LnCap labelled tumor cells (16X): background subtraction and median filtering (D), binary thresholding (E), watershed segmentation (F).

In conclusion, we have shown that the co-culture of tumor cells with primary fibroblasts, might lead to either growth stimulation or growth inhibition of tumor cells. Fibroblasts derived from the prostate of patients diagnosed with prostate carcinoma (potential CAFs) were the least inhibiting and occasionally even promoting tumor proliferation. Fibroblasts derived from the skin of pediatric patients, were highly represented in the group of the most inhibitory fibroblasts.

Our high-throughput study, with over five hundred heterotypic cell combinations, with four independent measurements for each sample and individual counting of each tumor cell, indicates that the effect of fibroblasts on tumor cell proliferation is predominantly inhibitory. The technique allowed us to identify fibroblasts with consistently high and with consistently low inhibitory capacity. These findings are valuable to use in further studies trying to understand the mechanisms behind inhibition and its possible clinical relevance. Our data may reflect part of the fibroblast mediated microenvironmental control of tumor cell growth.

Whether our *in vitro* neighbour suppression results would correlate with cancer proneness of the donors remains to be established. However if such correlations would exist, our assay might provide an easy and highly scalable tool to test the inhibitory activity on population levels. The assay may also permit the dissection of the mechanism of inhibition by high throughput tools where large number of agents (drugs, siRNA, antibodies) can be tested for enhancing or abolishing the inhibitory effects of the fibroblasts.

3.6 PAPER VI

The differential inhibition of tumor cells by normal and cancer-derived fibroblasts is dependent on the architecture of the fibroblast monolayer

As a first attempt to dissect the mechanism of contact mediated inhibition, the aim of Paper VI was to investigate the role of the architecture of the fibroblast monolayer.

In the previous study (Paper V), we demonstrated that monolayers of a panel of hundred primary fibroblasts could differentially inhibit tumor cell proliferation *in vitro*. In the course of 500 co-culture experiments, we observed a clear difference in the growth pattern of the tumor cells growing on top of fibroblasts with different inhibitory capacity. In the inhibited cultures, the tumor cells grew in small confined islands (Figure 3.6.1 A-B and Figure 1A, Paper VI). Tumor cells growing on non-inhibitory fibroblasts grew in bigger islands and showed a more dispersed pattern (Figure 3.6.1 C-D and Figure 1B, Paper VI).

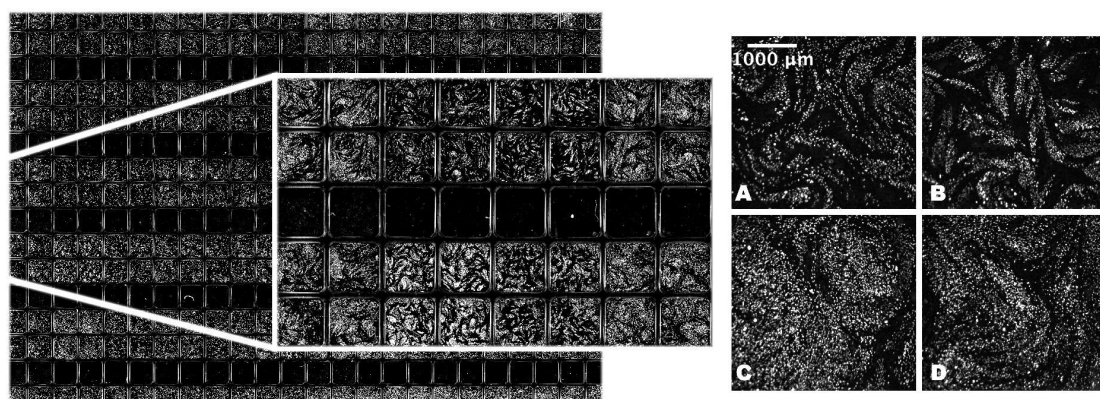


Figure 3.6.1 Bird-eye view of fibroblast monolayers in a 384-well plate + zoom in on single wells: mRFP-labelled PC3 tumor cells growing on top of fibroblast monolayers with different inhibitory capacity. Growth pattern of tumor cells, after 4-days co-culture, on top of two inhibitory fibroblasts; Normal patient 1 skin (A) and BjhTERT (B) and on top of two non-inhibitory fibroblasts; Cancer patient 2 prostate (C) and Normal patient 1 hernia (D).

A morphological difference between inhibitory and non-inhibitory fibroblasts could also be observed when fibroblasts were cultured alone. The inhibitory fibroblasts appeared to grow in an organized “whirly” pattern, while non-inhibitory fibroblasts tended to arrange themselves in a “crossy” pattern. Our co-culture data suggested that the growth pattern of the tumor cells reflected the architecture of the underlying fibroblasts.

We selected, for further investigation, four fibroblasts that were identified as inhibiting and less-inhibiting in Figure 5, Paper V. One of the least inhibiting prostate fibroblasts “Ö15p2 AdInt” (Cancer patient 2 prostate) and one of the most inhibiting pediatric skin fibroblasts “D6MKsk PedSk” (Normal patient 1 skin) were selected from Figure 6, Paper V. “D6MKin PedInt” (Normal Patient 1 hernia) fibroblasts were selected from the less inhibiting fibroblasts in Figure 5, Paper V. In addition, telomerase immortalized BjhTERT fibroblasts were also selected as a stable inhibitor (Figure 5, Paper V).

We showed that the differences in the inhibitory capacity of normal skin derived fibroblasts, as contrasted to non-inhibitory prostate and hernia derived fibroblasts, are reproducible and did not depend on the initial number of tumor cells seeded (range 50–800 tumor cells) (Figure 2A, Paper VI). The inhibitory effect was also shown to be independent of the fibroblast passage number (passages 7, 8 and 14) (Figure 2B, Paper VI).

Choosing BjhTERT/mRFP-PC3 as a stable model system, we measured the inhibitory effect of different ages of monolayer. We showed that the inhibitory capacity increased significantly between two and four days old monolayer suggesting that certain components of the monolayer needed to mature in order to exert a strong inhibitory effect (Figure 5A-C, Paper VI). Again we confirmed that the inhibitory effect could not be explained solely by soluble factors. Supernatant from 8, 6, 4 and 2 days old fibroblasts cultures had no effect on the proliferation of tumor cells, independent on the origin of the supernatant. Careful examination of the microscopy image in Figure 5D, Paper VI revealed that fibroblasts mixed with tumor cells in the “0 days” old monolayer had no effect on tumor cell proliferation nor on the tumor growth pattern, i.e. the tumor cells grew in patterns identical to the controls. In Figure 6 Paper VI, we also observed that interference with monolayer formation impaired inhibition. These data clearly showed that it was not sufficient to have the inhibitory fibroblast present in the mixed cell culture, but that they also had to form a confluent and sufficiently matured intact monolayer to exert the inhibitory effect. Our data suggested that structured accumulation and deposition of extracellular matrix molecules might provide orientation dependent behavioral cues to the tumor cells in an unmanipulated, inhibitory monolayer.

We used time-lapse imaging combined with extended field capture (as described in Paper 1, and Paper VI modified for the Microscope platform 2) to investigate the continuous behavior of tumor cells growing on fibroblast monolayers. We recorded a movie during 62.5 hours with 49 (7x7) images covering a total area of 4.2 mm x 5.2 mm (22 mm²), captured every 15 minutes. A BjhTERT fibroblast monolayer, with strong inhibitory effect on tumor cell proliferation (Figure 5 & Figure 7A, Paper VI), was found to reduce the motility of the tumor cells during the 62.5 hours long movie (Figure 7B, Paper VI). The monolayer from hernia fibroblasts (normal patient 1) on the other hand, had no effect on tumor cell motility (Figure 7B, Paper VI) and allowed continuous tumor cell proliferation throughout the time of filming (Figure 7A, Paper VI). The finding that growth inhibition was associated with loss of motility along the surface of the inhibitory monolayer but not on a non-inhibitory monolayer indicated the occurrence of adhesive interactions in the former case that could impose cellular polarity. Non-inhibitory cultures might lack the cell surface molecules or the ECM components needed for adhesive interactions, permitting the continuous rolling of tumor cells over the monolayer and preventing the induction of eventual polarity.

RNA-profiling of two isogenic pairs of fibroblasts; the whirly and crossy subclones of the TERT immortalized line (BjhTERT) and skin (inhibitory) and hernia (non-inhibitory) fibroblasts derived from the same patient (Normal patient 1), identified a set of genes that co-segregated with the inhibitory phenotype. This suggests that our model system may

reveal molecular mechanisms involved in contact-mediated microenvironmental surveillance that may protect the organism from the outgrowth of disseminated tumor cells. We are now aiming at the characterization of the behavior of some of these candidate molecules in order to gain further insights into the molecular mechanisms of fibroblast monolayer induced tumor growth inhibition.

5. CONCLUDING REMARKS AND FUTURE PERSPECTIVES

The ambition of this thesis was to develop and implement automated microscopy methods into tumor biology research that can potentially be of clinical use. We have developed a set of computer programs that were able to carry out automated image capture on different types of motorized fluorescence microscopes. In addition, we have designed image analysis routines in order to automatically process and quantitate raw image data. Using a flexible programming environment, we have applied the acquisition and analysis routines for several different experimental settings, in order to answer different biological questions. By combining image acquisition and image analysis steps in the same algorithm, we could approach intelligent microscope applications where the system can decide how to proceed with the image acquisition depending on what the microscope “sees”.

We have demonstrated that using our automated microscopy methods it is possible to:

- produce seamless confocal and wide-field panoramas of tissue sections, embryos or isolated cells. The high throughput digitization of biological material is the prerequisite of virtual microscopy.
- perform quantitative analysis of thousands of cells growing sparsely or in monolayers on microscope slides or on 384-well plates

Our automated microscopy method has been applied in several different research projects (see related publications). The work presented in this thesis illustrated two types of projects that would not have been possible to carry out without this technique:

- i) characterization of drug sensitivity profiles of tumor cells and to measure the effect of anti-cancer drugs on immune effector cells (Paper III and IV)
- ii) measuring the effect of a large panel of human fibroblasts on the proliferation of tumor cells in mixed cell cultures (Paper V and Paper VI)

The two drug sensitivity studies laid the ground for an extensive ongoing project that aims to provide tools for assay guided individualized treatment of cancer patients. We have developed an assay for primary tumor cells (iVV – *in vitro* viability assay), which addresses many of the shortcomings and limitations of the previous drug sensitivity assays. Using custom built hardware and our own capturing and analysis software, we have managed to create a robust, reliable and affordable system. During the past five years, our group has carried out almost 500 drug sensitivity tests on primary tumor cells, with a minimum of 30 different drugs.

In summary, this method allowed us to draw three simple conclusions (Figure 2.7 – 2.8):

- (i) there are no drugs that work on all tumors, (ii) all drugs can be effective against certain tumors and (iii) very resistant tumors can still be sensitive for a few drugs.

In the future, the assay will also be adapted to test sensitivity of solid tumors. It will be used to explore the possibility to find suitable tumor targets for newly developed anti-cancer drugs. The assay may also provide new possibilities for patient pre-selection in clinical trials both for new drugs, or for new use of already licensed drugs.

The introduction of high throughput time-lapse imaging of mixed cell cultures opened up new ways to study tumor–effector interactions in a parallel fashion. The use of chemical or genetic fluorescence labels to identify the target cells at the beginning and at the end of the experiment allowed us to collect quantitative information about cell viability and proliferation rates even when working at low cell numbers or analysing heterogeneous populations. This experimental set-up permitted us to revisit some old questions concerning microenvironmental control of tumor cell growth. Even though “Paget’s seed and soil hypothesis” dates back to 1889, the molecular determinants of the seed are still much better understood than those of the soil” (Fidler 2003; Mueller and Fusenig 2004). Almost 50 years have elapsed since Michael Woodruff reported on an exceptional patient that indicated the existence of some radiosensitive microenvironmental control of dormant tumor cells (Woodruff 1982). Furthermore, it was 45 years ago that Michael Stoker provided experimental evidence that normal murine fibroblasts can interfere with the proliferation of their transformed derivatives (Stoker 1964; Stoker, Shearer et al. 1966). But only now can we address, with the help of new technologies, the possible mechanism behind the phenomenon.

Concerning the relevance of the *in vitro* observed fibroblast mediated tumor growth inhibition many questions remains to be answered:

- how is the contact dependent inhibition mediated?
- is there analogous inhibitory effect *in vivo*?
 - if YES - Is there any difference between individuals in their capacity to suppress tumor cell growth through microenvironmental control?
 - if YES - How can it be measured most effectively?
 - if YES - Is it possible to boost it pharmacologically in cancer patients to prevent additional spreading of the tumor? Can it be boosted as a preventive measure in individuals with high tumor risk?

Is our *in vitro* co-culture system sensitive enough to design assays that can identify the molecular mechanism that control the fibroblast mediated inhibition or to use it to identify pharmacological agents that can enhance its activity?

The introduction of microscopy into classical biology was groundbreaking and ever since, each new type of microscopy technique has contributed to big steps in the understanding of biology. The advent of automated microscopy techniques, into selected laboratories, in combination with the computational power of almost any computer today, already represents giant leaps in the field of visualizing biology.

This thesis has illustrated that the combination of available and affordable techniques allowed us to carry out microscopy experiments that were previously only possible to do in specialized high throughput image facilities or in the pharmaceutical industry.

6. METHODOLOGICAL CONSIDERATIONS

6.1 PRIMARY FIBROBLAST CULTURES – TRICKS AND TIPS

Primary fibroblast cultures were established from mechanically dissociated tissue pieces. Tissue from surgical rest materials, prostate fine needle biopsies and skin punch biopsies were transported from the clinics, overnight at room temperature, in Iscove's modified Dulbecco's medium (IMDM) supplemented with 10% heat-inactivated fetal bovine serum (FBS) and penicillin, streptomycin and gentamicin at 100, 100 and 50 µg/mL concentration, respectively (PSG additive). Upon arrival the material was rinsed in phosphate buffered saline (PBS). Surgical rest materials and skin biopsies were put through 2 or 3 washes of PBS to be cleaned sufficiently. Transferring the pieces to new culture dishes containing PBS most easily does washing. Using a sterile surgical blade and forceps the tissue was gently cut into smaller pieces and forced to adhere to thin scratches made in the plastic bottom of the dish (3.5, 6 or 10 cm culture dish). It is wise to divide the material in at least two separate dishes, to prevent entire loss if fungus or bacteria infect one dish. To prevent the material from floating around during the dissociation and adherence procedure, only a drop of medium should cover the tissue pieces. At the end, 2-10 ml culture medium (IMDM, 10-20% FBS, PSG) should carefully be added to the dish so as not to dislodge the pieces from the plastic surface. It is optimal to store the dishes in a plastic box in the incubator, without moving it around or changing the medium for 4-5 days. The first cells should be seen within 10-14 days of culturing.

To improve the expansion of very small islands of outgrowths or sparsely and slowly growing cells the IMDM medium could be supplemented with fibroblast growth medium (FGM, including fibroblast growth supplements (FGS)) in 4:1 ratio of IMDM:FGM, 10-20% FBS, PSG. To prevent apoptosis induced by oxidative stress at low cell density, the medium could also be enriched with the antioxidant mix of sodium pyruvate, α -thioglycerol and bathocuproine disulfonate (Brielse, Bechet et al. 1998).

6.2 PROGRAMMING IN OPENLAB AUTOMATOR – NUTS AND BOLTS

We have used the visual programming environment of OpenlabAutomator to develop programs for automated image capture and image analysis. The concept of visual programming, with icons linked into flowcharts is illustrated below by the Moving-Z capture loop and Get automator time loop (Figure 6.2.1-6.2.2). Figure 6.2.3 A-C show bird-eye-view images of the three programs developed in this thesis; QuantCapture 4.0, QuantCount 3.0 and CytotoxCount 3.0.

Moving Z-capture loop:

The true (T) or false (F) icon contains an if-statement for a certain wavelength of illumination. If the user has preset an exposure time for this wavelength the statement does not equals zero and the statement is therefore true and T-links will direct the flow into the loop of the moving Z capture. If it is zero, meaning that this wavelength is not included in the capture the statement is regarded as false and the F-link take the command to the next T/F-wavelength icon (Figure 6.2.1). If selected, the loop will open the shutter and move the z-stage simultaneously for the length of time defined by "get automator-time"-loop.

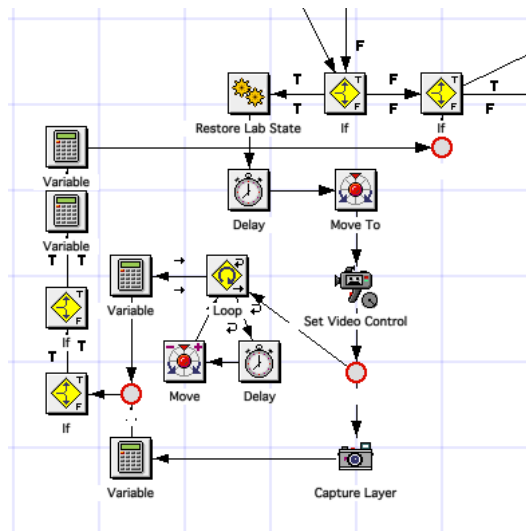


Figure 6.2.1 Moving Z-capture loop

Quantcapture_4 - Get automator time & capture Dark background

Synchronization loop: The Moving Z-capture requires the exposure time of the camera to be precisely synchronized with the time it takes to move through the Z-stack. This time is dependent on sample z-thickness, number of z-steps and the exposure for different wavelengths. A dummy capture calculates the exposure time plus the travel time and capture simultaneously a “dark background” image (using closed shutters) for the total exposure time (inclusive Z-travel). This “dark background” image will later be re-used to subtract camera noise from the raw Moving Z-image (Figure 6.2.2).

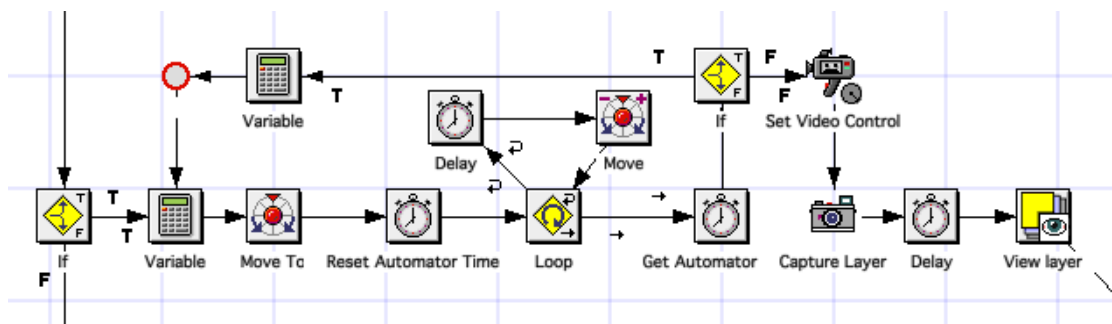


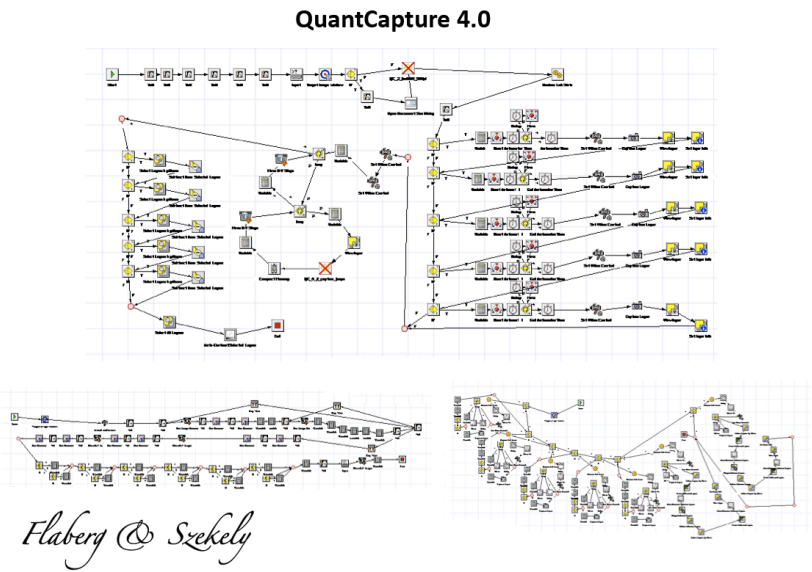
Figure 6.2.2 Get automator-time loop

6.3 IMAGE PROCESSING/ANALYSIS - COMMENTS

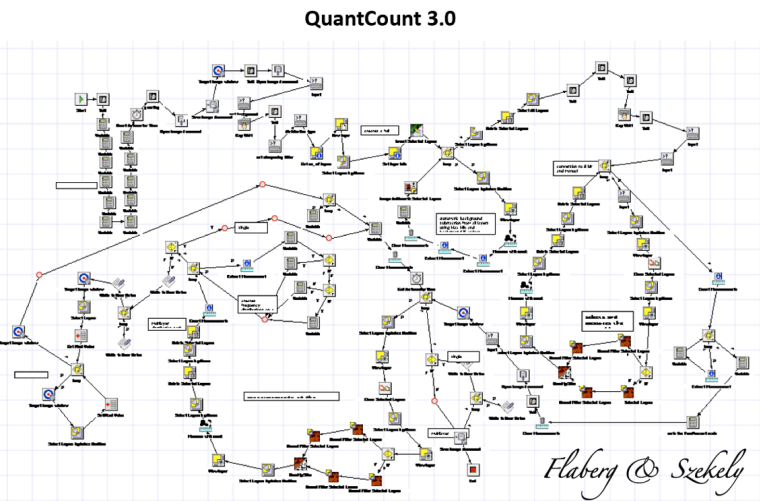
There is no general “theory” of image enhancement. When an image is processed for visual interpretation, the viewer is the ultimate judge of how well a particular method works (Gonzalez and Woods 2008). This is important to remember in image processing, because with freedom comes responsibility. Any change made to the image must be applied uniformly to the whole image and to all images inside the image-stack/experiment, including controls. Changes must be documented and the original raw image must always be saved, in a lossless file format. Reviewers always have the right to claim visual inspection of original, raw image files.

Figure 6.2.3

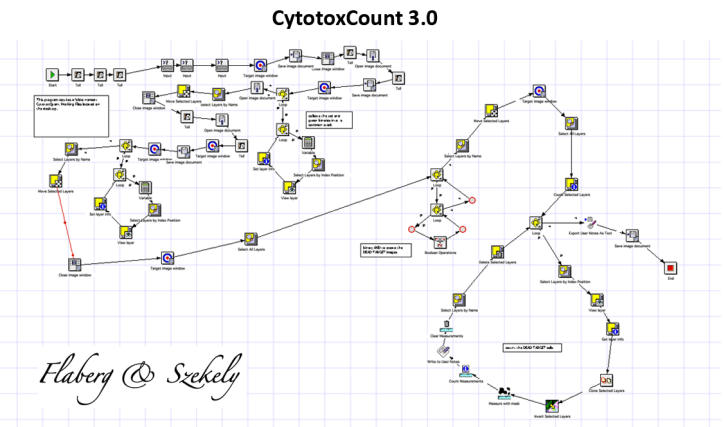
A



B



C



7. ACKNOWLEDGEMENTS

I would like to express my gratitude to the Karolinska Institutet and to the Department of Microbiology, Tumor and Cell biology (MTC), where the work of this thesis was performed.

Thank you to all the people who have made this possible.

Laszlo Szekely, my supervisor. This has been the greatest adventure of my life. When **Anna Szeles** first introduced you to me, the “Microscope guru of MTC”, I remember thinking: I will never understand everything he says. I will never fluently speak that language of technical terms and acronyms, and so fast. Two days after our first encounter and discussion in the C3-corridor I was already working with you opening the boxes and unwiring the wires that later became the first automated microscope set-up that we built. Your generosity to share your knowledge, your support and your never-ending belief in me has helped me become the researcher I am today. Now, I can speak the language and I see molecular abbreviations on the number plates of cars. Well, I did already speak fast before I met you.

Georg Klein, I am grateful for having the chance to work with you, for your guidance through the years of my thesis and for introducing me to wonders of science. Your wisdom and insights have taught me many things about science and how to be a good scientist. Thank you for your support and belief in me.

My co-supervisors: **Åsa Gustafsson-Jernberg**, **Valdas Pasiskevicius** and **Sven Hoffner**. Thank you for discussions and great support. I knew that I could always ask you if I had any questions. My mentor, **Carl Johan Sundberg**. Thank you for good advice, inspiration and fighting spirit.

I have had the best co-worker’s possible. Thank you for always being there! To my science-soul-sisters: **Ms Fibroblast Tatiana Pavlova**, **Orsolya Réka Muhari** and **Rita Hutyra-Gram Ötvös**, thank you for all the fun wet lab-moments and company feeding cells late into the nights. **Laszlo Markasz** (thank you for great work together), **Gabor Petranyi** and **Gyuri Stuber**, I really enjoyed working with you and it was empty when you left. **Hayrettin Guven**, thank you for your devotion for our project and fun discussions. **Andrej Savchenko**, thank you for sharing your great knowledge in microscopy, physics and electronics, anytime I ask. **Kenth Andersson**, thank you for being around when extra hands were needed. **Barbro Elin Henriksson** och **Mia Lövbeer**, thank you for always being a calming force to count on upstairs, and for all the help with small and big things.

Elena Kashuba, thank you for nice discussions, hugs and chocolate. **Suhas Dareka** and **Sree Harsha Gurrapu** thank you for nice lab-company! **Vladimir Kashuba** for bringing additional knowledge to us. **Henriette Skribek**, thank you for your kind support.

The C3-corridor. I can’t imagine a better corridor to work in! You have all contributed to warm, fun and inspiring working environment. **Sonia Lain** and her group members are the first ones to greet me with a smile or a nice chat in the morning (thanks to you **Anna McCarthy**, **Marijke Sachweh**, **Catherine Drummond** and **Ingeborg van Leeuwen**). Correction, probably the second smile I would receive if I went through the reception – thank you **Birgitta Wester**, **Greger Blomqvist**, **Sandor Feldötö**, and **Torbjörn Lager** for help over the years. Next up in the corridor are the CIM Northers, **Benedict Chambers** and **Adnane Achour**; thank you for your friendship, support and the many laughs. Thank you **Adil Duru** for lab company at the most odd hours and to **Eva Allerbring** and **Hannes**

Uchtenhagen. To all the members of the **Klas Kärre's** and **Petter Höglund's** groups. Thank you for smiles at the end of the corridor. In particular to **Hanna Kakis Brauner**, it was so nice to have you around and I miss our science chats! And to **Rossana Tallerico** and **Arneka Wagener** for great Italian/German/American spirit!

Thank you to all my friends and colleagues at MTC and SMI, past and present. Thanks for contributing to the nice research environment. **Gerry McInerney** for friendship and support, **Dani Bada** for your Catalanian hugs, **Jakob Lovén** for the nice chats about science and stuff – and for recommending me the best printers!, **Keira Melican** for sharing a passion for microscopy, **Jessica Kennedy Weidner** for sharing a passion for dogs, **Björn Önfelt**, **Bruno Vanherberghen** and **Michael Uhlin** for fun collaboration and discussions, **Melissa Norström**, **Carina Perez**, **Li-Sophie Rathje**, **Anna-Maria Birgersdotter**, **Hanna Zirath**, **Frank Heuts**, **Noemi Nagy**, **Pegah Rouhi**, **Elizabeth Hellström** and **Stefano Sammiceli** for being such nice people to run into everyday. **Mikael Jondahl** and **Katalin Benedek** for great interactions at KIVIF. **Martin Rottenberg**, **Stefan Imreh**, **Gunilla Karlson**, **Anders Örn**, **Rolf Olsson**, **Anneka Ernst**, **Maria Masucci**, **Galina Selivanova**, **Lars-Gunnar Larsson** and **Francesca Chiodi** thanks for the contacts over the years. Thanks to **Åsa Szekely Björndahl** for encouragement and support! Thank you **Eva Klein** for your passion in tumor biology and for sharing insights in life and science. **Ingemar Ernberg**, thank you for your devotion in science and the exciting What is life course! Thank you **Anita Wallentin** and **Anna Lögdberg** for administrating us students and also thank you to **John Sennett**.

To colleagues outside MTC. Thank you **Hans Blom** for all support and knowledge in microscopy and physics that you so generously shared, **Sara Abrahamsson** and **Emilie Louvet** for entering the world of image analysis with me and for company on microscopy conferences around the world (from Krakow and Shanghai to Konstanz), **Magnus Lindskog** and **Lars Karlsson** for sharing the passion in medicine with me. **Gilles Carpentier** for your generous advice regarding image analysis. **Lennart Nilsson**, thank you for sharing your art and love for microscopy with me. Thank you, **Mikael Agaton** and **Tom Brass** for making beautiful science for TV. Thank you **Mina Bissell** for your friendship and your passion for science. You always give me inspiration.

I am grateful to all collaborators for fruitful work and interesting discussions. Thank you! **Elias Arnér**, **Stefanie-Prast Nilsen**, **Sofie Eriksson**, **Mats Wahlgren**, **Ulf Ribacke**, **Lorand Levente Kis**, **Klas Wiman**, **Nina Rökaeus**, **Yihai Cao**, **Renhai Cao**, **Per Sabelström**, **Christer Strand**, **Arne Östman**, **Martin Augsten**, **Per Hall**, **Jingmei Li**, **Staffan Eksborg**, **Pontus Aspenström**, **Annica Gad**, **Alejandra Vasquez**, **Ennio Carbone** and **Tobias Olsson**. I would like to especially thank the **doctors, nurses and patients** who have contributed with invaluable material, in several of the studies in this thesis. In particular, **Swen-Olof Andersson**, **Jan-Erik Johansson**, **Ove Andrén**, **Irene Petterson**, **Mikaela Luthman**, **Richard Skröder**, **Ulla Zachrisson** and **Carl Johan Fürst**.

I am so thankful for all the wonderful friends I also have outside KI. You all mean a lot to me. **Frida Hesselgren**, **Fredrik Olsson**, **Helena Forsén**, **Maria Söderström**, **Malin Belfrage** and **Rebecca Lagerkvist**. Thank you for being the best friends that I could ever wish for.

To my dear family, my mother **Kjerstin**, my father **Thomas**, my sister **Pauline** and my grandmother **Inga**. Thank you for your endless support, love and belief in me.

Magnus Jökulsson. Thank you for being there. Ég ást þú.

8. REFERENCES

- Ablett, S., F. Doz, et al. (2004). "European collaboration in trials of new agents for children with cancer." *Eur J Cancer* **40**(12): 1886-1892.
- Alberts, B., B. Johansson, et al. (2002). *Molecular biology of the cell*, Garland science.
- Allard, D., M. Stoker, et al. (2003). "A G2/M cell cycle block in transformed cells by contact with normal neighbors." *Cell Cycle* **2**(5): 484-487.
- Allen, M. and J. Louise Jones (2011). "Jekyll and Hyde: the role of the microenvironment on the progression of cancer." *J Pathol* **223**(2): 162-176.
- Barbe, L., E. Lundberg, et al. (2008). "Toward a confocal subcellular atlas of the human proteome." *Mol Cell Proteomics* **7**(3): 499-508.
- Barton, S. and C. Swanton (2011). "Recent developments in treatment stratification for metastatic breast cancer." *Drugs* **71**(16): 2099-2113.
- Beliveau, A., J. D. Mott, et al. (2010). "Raf-induced MMP9 disrupts tissue architecture of human breast cells in three-dimensional culture and is necessary for tumor growth in vivo." *Genes Dev* **24**(24): 2800-2811.
- Bertelsen, C. A., V. K. Sondak, et al. (1984). "Chemosensitivity testing of human solid tumors. A review of 1582 assays with 258 clinical correlations." *Cancer* **53**(6): 1240-1245.
- Bissell, M. J. and W. C. Hines (2011). "Why don't we get more cancer? A proposed role of the microenvironment in restraining cancer progression." *Nat Med* **17**(3): 320-329.
- Bissell, M. J. and D. Radisky (2001). "Putting tumours in context." *Nat Rev Cancer* **1**(1): 46-54.
- Bower, M. (2002). "The management of lymphoma in the immunosuppressed patient." *Best Pract Res Clin Haematol* **15**(3): 517-532.
- Bozic, I., T. Antal, et al. (2010). "Accumulation of driver and passenger mutations during tumor progression." *Proc Natl Acad Sci U S A* **107**(43): 18545-18550.
- Bravo-Zanoguera, M. E., C. A. Laris, et al. (2007). "Dynamic autofocus for continuous-scanning time-delay-and-integration image acquisition in automated microscopy." *J Biomed Opt* **12**(3): 034011.
- Bredberg, A. (2009). "Cancer resistance and Peto's paradox." *Proc Natl Acad Sci U S A* **106**(20): E51; author reply E52.
- Briemeier, M., J. M. Bechet, et al. (1998). "Improving stable transfection efficiency: antioxidants dramatically improve the outgrowth of clones under dominant marker selection." *Nucleic Acids Res* **26**(9): 2082-2085.
- Brown, L. F., A. J. Guidi, et al. (1999). "Vascular stroma formation in carcinoma in situ, invasive carcinoma, and metastatic carcinoma of the breast." *Clin Cancer Res* **5**(5): 1041-1056.
- Campbell, R. E., O. Tour, et al. (2002). "A monomeric red fluorescent protein." *Proc Natl Acad Sci U S A* **99**(12): 7877-7882.
- CancerResearchUK and IARC. (2011). "CancerStats – Cancer Worldwide: http://publications.cancerresearchuk.org/downloads/Product/cs_pdf_worldwide_2011.pdf." Retrieved 2011-11-25, 2011.
- Caulin, A. F. and C. C. Maley (2011). "Peto's Paradox: evolution's prescription for cancer prevention." *Trends Ecol Evol* **26**(4): 175-182.
- Cerwenka, A. and L. L. Lanier (2001). "Natural killer cells, viruses and cancer." *Nat Rev Immunol* **1**(1): 41-49.

- Chang, H. Y., J. T. Chi, et al. (2002). "Diversity, topographic differentiation, and positional memory in human fibroblasts." Proc Natl Acad Sci U S A **99**(20): 12877-12882.
- Chen, G. G. and P. B. S. Lai (2009). Apoptosis in Carcinogenesis and Chemotherapy Apoptosis in cancer, Springer.
- Chi, K. R. (2009). "Super-resolution microscopy: breaking the limits." Nature Methods **6**, **15 - 18** (2009)(6): 15 - 18.
- Coca, S., J. Perez-Piqueras, et al. (1997). "The prognostic significance of intratumoral natural killer cells in patients with colorectal carcinoma." Cancer **79**(12): 2320-2328.
- Conchello, J. A. and J. W. Lichtman (2005). "Optical sectioning microscopy." Nat Methods **2**(12): 920-931.
- Conrad, C., H. Erfle, et al. (2004). "Automatic identification of subcellular phenotypes on human cell arrays." Genome Res **14**(15173118): 1130-1136.
- Conrad, C., A. Wunsche, et al. (2011). "Micropilot: automation of fluorescence microscopy-based imaging for systems biology." Nat Methods **8**(3): 246-249.
- Dobbie, I. M., E. King, et al. (2011). "OMX: a new platform for multimodal, multichannel wide-field imaging." Cold Spring Harb Protoc **2011**(8): 899-909.
- Dolberg, D. S. and M. J. Bissell (1984). "Inability of Rous sarcoma virus to cause sarcomas in the avian embryo." Nature **309**(5968): 552-556.
- Eggeling, C., C. Ringemann, et al. (2009). "Direct observation of the nanoscale dynamics of membrane lipids in a living cell." Nature **457**(7233): 1159-1162.
- Egner, A. A., V. Hell, S. W (2002). "Comparison of the axial resolution of practical Nipkow-disk confocal fluorescence microscopy with that of multifocal multiphoton microscopy: theory and experiment." Journal of Microscopy **Vol. 206**(Pt 1): 24 – 32.
- Erez, N., M. Truitt, et al. (2010). "Cancer-Associated Fibroblasts Are Activated in Incipient Neoplasia to Orchestrate Tumor-Promoting Inflammation in an NF-kappaB-Dependent Manner." Cancer Cell **17**(2): 135-147.
- Farkas, D. L., R. C. Leif, et al. (1999). Proceedings of optical diagnostics of living cells II : 25-26 January 1999, San Jose, California. Bellingham, Wash., USA, SPIE.
- Ferlay, J., H. Shin, et al. (2008). "GLOBOCAN 2008 v1.2, Cancer Incidence and Mortality Worldwide: IARC CancerBase No. 10 [Internet]." Retrieved Available from: <http://globocan.iarc.fr>, accessed on 20/10/2011., 2011.
- Ferlay, J., H. R. Shin, et al. (2010). "Estimates of worldwide burden of cancer in 2008: GLOBOCAN 2008." Int J Cancer.
- Fidler, I. J. (2003). "The pathogenesis of cancer metastasis: the 'seed and soil' hypothesis revisited." Nat Rev Cancer **3**(6): 453-458.
- Fields, B. N., D. M. Knipe, et al. (1996). Fields virology. Philadelphia, Lippincott-Raven Publishers.
- Fiske, J. (1990). Introduction to communication studies. Studies in culture and communication. London ; New York, Routledge: xvi, 203 p.
- Foulds, L. (1954). "The experimental study of tumor progression: a review." Cancer Res **14**(5): 327-339.
- Frigault, M. M., J. Lacoste, et al. (2009). "Live-cell microscopy - tips and tools." J Cell Sci **122**(Pt 6): 753-767.
- Glatz-Krieger, K., U. Spornitz, et al. (2006). "Factors to keep in mind when introducing virtual microscopy." Virchows Arch **448**(16362822): 248-255.
- Glick, A. B. and S. H. Yuspa (2005). "Tissue homeostasis and the control of the neoplastic phenotype in epithelial cancers." Semin Cancer Biol **15**(2): 75-83.
- Goel, S., D. G. Duda, et al. (2011). "Normalization of the vasculature for treatment of cancer and other diseases." Physiol Rev **91**(3): 1071-1121.

- Goetz, J. G., S. Minguet, et al. (2011). "Biomechanical remodeling of the microenvironment by stromal caveolin-1 favors tumor invasion and metastasis." Cell **146**(1): 148-163.
- Goldman, R. D., J. Swedlow, et al. (2010). Live cell imaging : a laboratory manual. Cold Spring Harbor, N.Y., Cold Spring Harbor Laboratory Press.
- Gonzalez, R. C. and R. E. Woods (2008). Digital image processing. Upper Saddle River, NJ, Pearson/Prentice Hall.
- Gustafsson, A., V. Levitsky, et al. (2000). "Epstein-Barr virus (EBV) load in bone marrow transplant recipients at risk to develop posttransplant lymphoproliferative disease: prophylactic infusion of EBV-specific cytotoxic T cells." Blood **95**(3): 807-814.
- Gustafsson, M. G. L. (2000). "Surpassing the lateral resolution limit by a factor of two using structured illumination microscopy." Journal of Microscopy-Oxford **198**: 82-87.
- Hammond, A. T. and B. S. Glick (2000). "Raising the speed limits for 4D fluorescence microscopy." Traffic **1**(12): 935-940.
- Hanahan, D. and R. A. Weinberg (2000). "The hallmarks of cancer." Cell **100**(1): 57-70.
- Hanahan, D. and R. A. Weinberg (2011). "Hallmarks of cancer: the next generation." Cell **144**(5): 646-674.
- Hardin, J. (2006). Confocal and Multi-Photon Imaging of Living Embryos. New York, 2006, SpringerScience+Business Media, New York, 2006.
- Haugland, R. P. (2005). The Handbook: A guide to Fluorescent Probes and Labeling Technologies, Invitrogen Group 2005.
- Hayon, T., A. Dvilansky, et al. (2003). "Appraisal of the MTT-based assay as a useful tool for predicting drug chemosensitivity in leukemia." Leuk Lymphoma **44**(11): 1957-1962.
- Heintzmann, R., T. M. Jovin, et al. (2002). "Saturated patterned excitation microscopy - a concept for optical resolution improvement." Journal of the Optical Society of America a-Optics Image Science and Vision **19**(8): 1599-1609.
- Hell, S. W. and J. Wichmann (1994). "Breaking the Diffraction Resolution Limit by Stimulated-Emission - Stimulated-Emission-Depletion Fluorescence Microscopy." Optics Letters **19**(11): 780-782.
- Hirsch, J. (2006). "An anniversary for cancer chemotherapy." JAMA **296**(12): 1518-1520.
- Hsieh, A. C. and M. M. Moasser (2007). "Targeting HER proteins in cancer therapy and the role of the non-target HER3." Br J Cancer **97**(4): 453-457.
- Inoue, S. (2006). Foundations of Confocal Scanned Imaging in Light Microscopy. New York, 2006, SpringerScience+Business Media, New York, 2006.
- Ishigami, S., S. Natsugoe, et al. (2000). "Prognostic value of intratumoral natural killer cells in gastric carcinoma." Cancer **88**(3): 577-583.
- Itoh, M., C. M. Nelson, et al. (2007). "Rap1 integrates tissue polarity, lumen formation, and tumorigenic potential in human breast epithelial cells." Cancer Res **67**(10): 4759-4766.
- JAMA (1963). "Percival Pott." JAMA **186**(November, 23): 795-796.
- Jemal, A., F. Bray, et al. (2011). "Global cancer statistics." CA Cancer J Clin **61**(2): 69-90.
- Joensuu, H. (2008). "Systemic chemotherapy for cancer: from weapon to treatment." Lancet Oncol **9**(3): 304.
- Kallioniemi, O. P., U. Wagner, et al. (2001). "Tissue microarray technology for high-throughput molecular profiling of cancer." Hum Mol Genet **10**(7): 657-662.
- Kalluri, R. and M. Zeisberg (2006). "Fibroblasts in cancer." Nat Rev Cancer **6**(5): 392-401.

- Karlsson, G., P. Nygren, et al. (2001). "Economic aspects of chemotherapy." Acta Oncol **40**(2-3): 412-433.
- Katz, P., A. M. Zaytoun, et al. (1982). "Mechanisms of human cell-mediated cytotoxicity. III. Dependence of natural killing on microtubule and microfilament integrity." J Immunol **129**(6): 2816-2825.
- Kieff, E. D. and A. B. Rickinson (2007). Epstein-Barr virus and its replication. In Fields' virology. Philadelphia, Wolters Kluwer Health/Lippincott Williams & Wilkins.
- King, R. D., J. Rowland, et al. (2009). "The automation of science." Science **324**(5923): 85-89.
- Klein, G. (2009). "Toward a genetics of cancer resistance." Proc Natl Acad Sci U S A **106**(3): 859-863.
- Klein, G. and P. Demant (2008). "Tumor Resistance." Cancer - The Outlaw Cell, 3rd Edition, Richard E LaFond, Editor, American Chemical Society Publication, in press.
- Klein, G., S. Imreh, et al. (2007). "Why do we not all die of cancer at an early age?" Adv Cancer Res **98**: 1-16.
- Lander, E. (2004). Lecture 34: Human Polymorphisms, MIT Introduction to Biology MIT Introduction to Biology, 7.012, MIT open courseware under a Creative commons licence.
- Larsson, R. and P. Nygren (1993). "Laboratory prediction of clinical chemotherapeutic drug resistance: a working model exemplified by acute leukaemia." Eur J Cancer **29A**(8): 1208-1212.
- Larsson, R. and P. Nygren (1993). "Prediction of individual patient response to chemotherapy by the fluorometric microculture cytotoxicity assay (FMCA) using drug specific cut-off limits and a Bayesian model." Anticancer Res **13**(5C): 1825-1829.
- Lauth, M. and R. Toftgard (2011). "Hedgehog signaling and pancreatic tumor development." Adv Cancer Res **110**: 1-17.
- Lee, S. H. (2005). "Virtual microscopy: applications to hematology education and training." Hematology **10 Suppl 1**: 151-153.
- Lemaire, M., S. Deleu, et al. (2011). "The microenvironment and molecular biology of the multiple myeloma tumor." Adv Cancer Res **110**: 19-42.
- Leong, F. J. and J. O. McGee (2001). "Automated complete slide digitization: a medium for simultaneous viewing by multiple pathologists." J Pathol **195**(11745684): 508-514.
- Lewin, N., P. Aman, et al. (1987). "Characterization of EBV-carrying B-cell populations in healthy seropositive individuals with regard to density, release of transforming virus and spontaneous outgrowth." Int J Cancer **39**(4): 472-476.
- Li, H., X. Fan, et al. (2007). "Tumor microenvironment: the role of the tumor stroma in cancer." J Cell Biochem **101**(4): 805-815.
- Lichtman, J. W. and J. A. Conchello (2005). "Fluorescence microscopy." Nat Methods **2**(12): 910-919.
- Lippincott-Schwartz, J. and G. H. Patterson (2003). "Development and use of fluorescent protein markers in living cells." Science **300**(5616): 87-91.
- Lo, W. Y. and S. M. Puchalski (2008). "Digital image processing." Vet Radiol Ultrasound **49**(1 Suppl 1): S42-47.
- Lock, J. G. and S. Stromblad (2010). "Systems microscopy: an emerging strategy for the life sciences." Exp Cell Res **316**(8): 1438-1444.
- Lozzio, B. B. and C. B. Lozzio (1979). "Properties and usefulness of the original K-562 human myelogenous leukemia cell line." Leuk Res **3**(6): 363-370.
- Lucitti, J. L. and M. E. Dickinson (2006). "Moving toward the light: using new technology to answer old questions." Pediatr Res **60**(16690954): 1-5.

- Lundberg, E., M. Gry, et al. (2008). "The correlation between cellular size and protein expression levels--normalization for global protein profiling." J Proteomics **71**(4): 448-460.
- Lundin, M., J. Lundin, et al. (2004). "A digital atlas of breast histopathology: an application of web based virtual microscopy." J Clin Pathol **57**(15563669): 1288-1291.
- Lynch, C. C. and L. M. Matrisian (2002). "Matrix metalloproteinases in tumor-host cell communication." Differentiation **70**(9-10): 561-573.
- Markasz, L., L. L. Kis, et al. (2007). "Hodgkin-lymphoma-derived cells show high sensitivity to dactinomycin and paclitaxel." Leuk Lymphoma **48**(17786721): 1835-1845.
- Markasz, L., H. Skribek, et al. (2008). "Effect of frequently used chemotherapeutic drugs on cytotoxic activity of human cytotoxic T-lymphocytes." J Immunother **31**(3): 283-293.
- Markasz, L., B. Vanherberghen, et al. (2008). "NK cell-mediated lysis is essential to kill Epstein-Barr virus transformed lymphoblastoid B cells when using rituximab." Biomed Pharmacother.
- McKnight, J. A. (2003). "Principles of chemotherapy." Clin Tech Small Anim Pract **18**(2): 67-72.
- Mintz, B. and K. Illmensee (1975). "Normal genetically mosaic mice produced from malignant teratocarcinoma cells." Proc Natl Acad Sci U S A **72**(9): 3585-3589.
- Morrison, D., S. Wolff, et al. (1995). Abell's Exploration of the Universe. Orlando, Florida John Vondeling, Saunders college publishing.
- Mueller, M. M. and N. E. Fusenig (2004). "Friends or foes - bipolar effects of the tumour stroma in cancer." Nat Rev Cancer **4**(11): 839-849.
- North, A. J. (2006). "Seeing is believing? A beginners' guide to practical pitfalls in image acquisition." J Cell Biol **172**(1): 9-18.
- Nygren, P., H. Fridborg, et al. (1994). "Detection of tumor-specific cytotoxic drug activity in vitro using the fluorometric microculture cytotoxicity assay and primary cultures of tumor cells from patients." Int J Cancer **56**(5): 715-720.
- Oheim, M. (2007). "High-throughput microscopy must re-invent the microscope rather than speed up its functions." Br J Pharmacol **152**(1): 1-4.
- Opelz, G. and B. Dohler (2004). "Lymphomas after solid organ transplantation: a collaborative transplant study report." Am J Transplant **4**(2): 222-230.
- Orazi, A., R. A. Hromas, et al. (1997). "Posttransplantation lymphoproliferative disorders in bone marrow transplant recipients are aggressive diseases with a high incidence of adverse histologic and immunobiologic features." Am J Clin Pathol **107**(4): 419-429.
- Ostman, A. and M. Augsten (2009). "Cancer-associated fibroblasts and tumor growth--bystanders turning into key players." Curr Opin Genet Dev **19**(1): 67-73.
- Otvos, R., H. Skribek, et al. (2011). "Drug sensitivity patterns of HHV8 carrying body cavity lymphoma cell lines." BMC Cancer **11**(1): 441.
- Pages, F., J. Galon, et al. (2010). "Immune infiltration in human tumors: a prognostic factor that should not be ignored." Oncogene **29**(8): 1093-1102.
- Parsonage, G., A. D. Filer, et al. (2005). "A stromal address code defined by fibroblasts." Trends Immunol **26**(3): 150-156.
- Partanen, J. I., A. I. Nieminen, et al. (2009). "3D view to tumor suppression: Lkb1, polarity and the arrest of oncogenic c-Myc." Cell Cycle **8**(5): 716-724.
- Partanen, J. I., A. I. Nieminen, et al. (2007). "Suppression of oncogenic properties of c-Myc by LKB1-controlled epithelial organization." Proc Natl Acad Sci U S A **104**(37): 14694-14699.

- Pepperkok, R. and J. Ellenberg (2006). "High-throughput fluorescence microscopy for systems biology." Nat Rev Mol Cell Biol **7**(9): 690-696.
- Perrotti, D. and P. Neviani (2008). "Protein phosphatase 2A (PP2A), a drugable tumor suppressor in Ph1(+) leukemias." Cancer Metastasis Rev **27**(2): 159-168.
- Prasher, D. C., V. K. Eckenrode, et al. (1992). "Primary structure of the Aequorea victoria green-fluorescent protein." Gene **111**(2): 229-233.
- Quintavalle, M., L. Elia, et al. (2011). "A cell-based high-content screening assay reveals activators and inhibitors of cancer cell invasion." Sci Signal **4**(183): ra49.
- Ramirez, C. N., T. Ozawa, et al. (2011). "Validation of a high-content screening assay using whole-well imaging of transformed phenotypes." Assay Drug Dev Technol **9**(3): 247-261.
- Rickinson, A. B., S. P. Lee, et al. (1996). "Cytotoxic T lymphocyte responses to Epstein-Barr virus." Curr Opin Immunol **8**(4): 492-497.
- Ross, J. C. (2011). The image processing handbook. Boca Raton, FL USA, CRC Taylor and Francis Group, LLC.
- Ross, M. H., G. I. Kaye, et al. (2002). Histology: A Text and Atlas, 4th edition, Lippincott Williams & Wilkins; Fourth Edition edition (October 15, 2002).
- Roussos, E. T., J. S. Condeelis, et al. (2011). "Chemotaxis in cancer." Nat Rev Cancer **11**(8): 573-587.
- Rowe, M., L. S. Young, et al. (1991). "Epstein-Barr virus (EBV)-associated lymphoproliferative disease in the SCID mouse model: implications for the pathogenesis of EBV-positive lymphomas in man." J Exp Med **173**(1): 147-158.
- Rubin, R., D. S. Strayer, et al. (2008). Rubin's Pathology : clinicopathologic foundations of medicine. Philadelphia, Lippincott Williams & Wilkins.
- Ruggeri, L., A. Mancusi, et al. (2006). "Natural killer cell recognition of missing self and haploidentical hematopoietic transplantation." Semin Cancer Biol **16**(5): 404-411.
- Sargent, J. M. (2003). "The use of the MTT assay to study drug resistance in fresh tumour samples." Recent Results Cancer Res **161**: 13-25.
- Sautes-Fridman, C., J. Cherfils-Vicini, et al. (2011). "Tumor microenvironment is multifaceted." Cancer Metastasis Rev **30**(1): 13-25.
- Schmidt, M. and H. Lipson (2009). "Distilling free-form natural laws from experimental data." Science **324**(5923): 81-85.
- Schulz, T. F. (2009). "Cancer and viral infections in immunocompromised individuals." Int J Cancer **125**(8): 1755-1763.
- Schwalbe, E. C., J. C. Lindsey, et al. (2011). "Rapid diagnosis of medulloblastoma molecular subgroups." Clin Cancer Res **17**(7): 1883-1894.
- Shimomura, O., F. H. Johnson, et al. (1962). "Extraction, purification and properties of aequorin, a bioluminescent protein from the luminous hydromedusan, Aequorea." J Cell Comp Physiol **59**: 223-239.
- Skribek, H., R. Otvos, et al. (2010). "Chronic lymphoid leukemia cells are highly sensitive to the combination of prednisolone and daunorubicin, but much less to doxorubicin or epirubicin." Exp Hematol **38**(12): 1219-1230.
- Slaga, T. J. (1983). "Overview of tumor promotion in animals." Environ Health Perspect **50**: 3-14.
- Starkuviene, V. and R. Pepperkok (2007). "The potential of high-content high-throughput microscopy in drug discovery." Br J Pharmacol **152**(1): 62-71.
- Stephens, D. J. and V. J. Allan (2003). "Light microscopy techniques for live cell imaging." Science **300**(5616): 82-86.
- Stoker, M. (1964). "Regulation of Growth and Orientation in Hamster Cells Transformed by Polyoma Virus." Virology **24**: 165-174.
- Stoker, M. G., M. Shearer, et al. (1966). "Growth inhibition of polyoma-transformed cells by contact with static normal fibroblasts." J Cell Sci **1**(3): 297-310.

- Stuber, G., K. Mattsson, et al. (2007). "HHV-8 encoded LANA-1 alters the higher organization of the cell nucleus." *Mol Cancer* **6**(17433107): 28-28.
- Sugimoto, H., T. M. Mundel, et al. (2006). "Identification of fibroblast heterogeneity in the tumor microenvironment." *Cancer Biol Ther* **5**(12): 1640-1646.
- Swedlow, J. R. (2011). "Finding an image in a haystack: the case for public image repositories." *Nat Cell Biol* **13**(3): 183.
- Tanjore, H. and R. Kalluri (2006). "The role of type IV collagen and basement membranes in cancer progression and metastasis." *Am J Pathol* **168**(3): 715-717.
- Terracini, B., J. W. Coebergh, et al. (2001). "Childhood cancer survival in Europe: an overview." *Eur J Cancer* **37**(6): 810-816.
- Tlsty, T. D. and L. M. Coussens (2006). "Tumor stroma and regulation of cancer development." *Annu Rev Pathol* **1**: 119-150.
- Ujhazy, P. and O. Babusikova (1991). "NK-cell activity affected by some cytostatic drugs and their additives." *Neoplasma* **38**(3): 303-312.
- Utsugi, T., S. Demuth, et al. (1989). "Synergistic antitumor effects of topoisomerase inhibitors and natural cell-mediated cytotoxicity." *Cancer Res* **49**(6): 1429-1433.
- Vajdic, C. M. and M. T. van Leeuwen (2009). "Cancer incidence and risk factors after solid organ transplantation." *Int J Cancer* **125**(8): 1747-1754.
- Varga, V. S., J. Bocsi, et al. (2004). "Scanning fluorescent microscopy is an alternative for quantitative fluorescent cell analysis." *Cytometry A* **60**(15229857): 53-62.
- Varner, J. A. and D. A. Cheresh (1996). "Integrins and cancer." *Curr Opin Cell Biol* **8**(5): 724-730.
- Wang, E., C. M. Babbey, et al. (2005). "Performance comparison between the high-speed Yokogawa spinning disc confocal system and single-point scanning confocal systems." *J Microsc* **218**(15857376): 148-159.
- Weaver, V. M. and P. Gilbert (2004). "Watch thy neighbor: cancer is a communal affair." *J Cell Sci* **117**(Pt 8): 1287-1290.
- Weinberg, R. A. (2008). "Coevolution in the tumor microenvironment." *Nat Genet* **40**(5): 494-495.
- Wetterstrand, K. (2011). "DNA Sequencing Costs: Data from the NHGRI Large-Scale Genome Sequencing Program." Retrieved Available at: www.genome.gov/sequencingcosts. Accessed [2011-10-25], 2011.
- White, J. G., W. B. Amos, et al. (1987). "An evaluation of confocal versus conventional imaging of biological structures by fluorescence light microscopy." *J Cell Biol* **105**(3112165): 41-48.
- Wirtz, D., K. Konstantopoulos, et al. (2011). "The physics of cancer: the role of physical interactions and mechanical forces in metastasis." *Nat Rev Cancer* **11**(7): 512-522.
- Wolf, D. E. (2007). "Fundamentals of fluorescence and fluorescence microscopy." *Methods Cell Biol* **81**: 63-91.
- Woodley, D. T., J. R. Stanley, et al. (1988). "Human dermal fibroblasts synthesize laminin." *J Invest Dermatol* **90**(5): 679-683.
- Woodruff, M. (1982). "The Walter Hubert Lecture, 1982. Interaction of cancer and host." *Br J Cancer* **46**(3): 313-322.
- Wright, G., B. Tan, et al. (2003). "A gene expression-based method to diagnose clinically distinct subgroups of diffuse large B cell lymphoma." *Proc Natl Acad Sci U S A* **100**(17): 9991-9996.
- Yang, J. and R. A. Weinberg (2008). "Epithelial-mesenchymal transition: at the crossroads of development and tumor metastasis." *Dev Cell* **14**(6): 818-829.
- Ying, X. and T. M. Monticello (2006). "Modern imaging technologies in toxicologic pathology: An overview." *Toxicol Pathol* **34**(7): 815-826.
- Zagris, N., A. E. Chung, et al. (2000). "Differential expression of laminin genes in early chick embryo." *Int J Dev Biol* **44**(7): 815-818.

- Zhou, X., F. Tian, et al. (2007). "Filamin B deficiency in mice results in skeletal malformations and impaired microvascular development." Proc Natl Acad Sci U S A **104**(17360453): 3919-3924.
- Zitvogel, L., O. Kepp, et al. (2010). "Integration of host-related signatures with cancer cell-derived predictors for the optimal management of anticancer chemotherapy." Cancer Res **70**(23): 9538-9543.